Solar Particle Observations from 24 January to 24 February 1967*

by

William G. Innanen**

A thesis submitted in partial fulfillment of the
requirements for the degree of Master of Science
in the Department of Physics and Astronomy
in the Graduate College of
The University of Iowa

February 1968

Thesis supervisor: Assistant Professor S. M. Krimigis

*Research supported in part by National Aeronautics and Space Administration under contract No. NAS5-9076

**NASA Trainee

Graduate College
The University of Iowa
Iowa City, Iowa

CERTIFICATE OF APPROVAL

MASTER'S THESIS

This is to certify that the Master's Thesis of

William G. Innanen

with a major in Physics has been approved by the Examining Committee as satisfactory for the thesis requirement for the Master of Science degree at the convocation of February 3, 1968.

Thesis committee: _____
Thesis supervisor

_____
Member

_____
Member

ACKNOWLEDGMENTS

I wish to thank Dr. S. M. Krimigis for his helpful suggestions and advice in the preparation of this thesis. I also wish to thank Dr. J. A. Van Allen for the reduction of the Mariner IV data, and Dr. A. J. Masley for the PCA data. Thanks are due also to Dr. T. P. Armstrong and Dr. E. C. Roelof for valuable discussions. The credit for the design, construction, and testing of the University of Iowa Explorer 33 experiment goes to Drs. T. P. Armstrong, S. M. Krimigis, and J. A. Van Allen, and the author gratefully acknowledges their work as well as the many others at the University of Iowa and elsewhere who aided them. I also wish to thank Mrs. Pamela Kostel for her excellent work in typing this thesis.

ABSTRACT

The period under study may be divided into three parts: (1) the 28 January event which persisted until 1 February, (2) a disturbed period from 1 February through 7 February, and (3) the 13 February event. The 28 January event was one of the larger events ever observed which had no visible source flare on the sun. Mariner IV, at the time of the 28 January flare, was located 82° west of the earth-sun line. The available data from Mariner IV indicates that there was a flux of protons with $E_p > 50$ MeV and a highly anisotropic flux of electrons with $E_e > 40$ keV present from 1642 to 2010 UT on 28 January. Explorer 33 at the earth observed no electrons and the observed flux of electrons was ~ 30% less than that observed by Mariner IV. Comparing this with areas of the sun that exhibited strong activity preceding or following this event, it was determined that the most probable position of the flare was 71° behind the east limb of the sun. During the disturbed period, the intensity-time profiles of the particle detectors were found to be very complex. Within this period, two distinct events occurred which were interpreted to consist of particles semi-trapped in an interplanetary magnetic field structure. The first at 1909 UT on 2 February was

found to consist of protons with $E_p > 10$ MeV. The second at 1542 UT on 4 February consisted of electrons with $E_e > 45$ keV. The onset of the 13 February event was observed at 1841 UT. This event was caused by an importance 3 flare occurring at 1749 UT. Most of the first portion of the event was obscured by a magnetospheric passage of Explorer 33. From 2342 UT on 15 February to 0848 UT on 16 February, the region of the interplanetary medium magnetically connected to the flare position was swept past the earth. From 0000 UT to 0500 UT on 16 February, a relative decrease in the number of alpha particles compared to the number of protons was noted. The ratio of the number of protons to alpha particles with energy per nucleon between 0.5 and 4.0 MeV/nucleon before, during, and after this period were 60 , 165, and 70, respectively. This is the first reported observation of such a variation.

TABLE OF CONTENTS

TABLE OF CONTENTS (CONT'D.)

TABLE OF TABLES

TABLE OF FIGURES

TABLE OF FIGURES (CONT'D.)

TABLE OF FIGURES (CONT'D.)

TABLE OF FIGURES (CONT'D.)

I. APPARATUS

A. Explorer 33

Explorer 33 was launched on 1 July 1966 into a highly eliptical orbit with a period of approximately 12 days. The orbit for the period under study is shown in Figure 1.

The satellite is "spin-stabilized" about an inertial direction with right assention 225° and declination - 21°, in celestial coordinates. The projection of this axis on the ecliptic plane is shown in Figure 1. The spin rate is approximately 26 rpm.

The University of Iowa experiment consists of four detectors:

(1) G1; an EON 6213 Geiger-Mueller tube with a 1.7 mg/cm^2 window,

(2) G2; an EON 6213 Geiger-Mueller tube with a 1.3 mg/cm^2 window,

(3) G3; an EON 6213 Geiger-Mueller tube with a 1.3 mg/cm^2 window,

(4) P1, 2, 3, 4; a 26.5 micron thick, totally depleted, silicon surface barrier detector with a surface area of of 10.4 mm^2.

The arrangement, energy thresholds, and other characteristics of these detectors are given in Table I.

The outputs of P1 and G1 (both perpendicular to the spin axis) are divided into four sectors with sector III centered on the sun. Thus, sectors I and III look in the antisolar and solar directions, respectively, and II and IV look at the ecliptic south and north, respectively.

Since G1 is sensitive to x-rays in the range ~ 2 to 12 Å, it is necessary to combine the four sectors of the detector in such a way that x-rays and particles are recorded separately. These two quantities are G1X and G1AV, where

$$G1X = G1(III) - \frac{1}{3}[G1(I) + G1(II) + G1(IV)]$$

and

$$G1AV = \frac{1}{3}[G1(I) + G1(II) + G1(IV)] .$$

Thus, for an isotropic particle flux and x-rays in sector III, G1X is the x-ray flux counted by G1 and G1AV is the spin-averaged particle flux. In the case of a strongly anisotropic particle distribution, the interpretation of G1X and G1AV is no longer clear. Since sector III is the sun centered sector, it is seen that for a particle distribution peaked within sector III, G1X will count

both x-rays and particles and GlAV will be lower than the true omnidirectional particle flux. An example of the latter was noted on 15 February. The Geiger tubes have side wall shielding sufficient to stop protons with $E_p \approx 60$ MeV.

The output pulses of the solid state detector are amplified and clipped to 200 nanoseconds. This short clipping time minimizes the possibility that two or more near-simultaneous pulses, which are individually below the threshold of the detector, will combine to produce one pulse sufficient to trigger the detector. Four pulse height discriminators are set to give the four pass-bands P1, P2, P3, and P4. The energy bands of these channels are given in Table I. P4 is set well above the maximum energy loss for protons entering through the collimator, and responds only to particles more massive than deuterons (which for this paper will be assumed to be alpha particles) if such particles are incident on the detector through the collimator. However, P4 can count protons which have sufficient energy ($E_p \gtrsim 60$ MeV) to penetrate the side wall shielding. The efficiency of the detector for penetrating protons is less than 0.1% [Krimigis and Van Allen, 1967]. The exact value of the efficiency depends strongly on the exact characteristics of the detector. The solid state detector is equipped with a small $_{95}Am^{241}$ source of alpha particles to provide assurance of its proper operation in flight.

The combination of detectors on Explorer 33 gives some information about electrons with energy $E_e \gtrsim 45$ keV, but cannot separately identify them from protons with energy $E_p \gtrsim 10$ MeV without additional information. The sampling rate for P1 sectors, G1 sectors, and P1 spin average is once every 81.81 seconds. G1 spin average, G2, G3, P2, P3, and P4 are sampled every 163.6 seconds.

B. Mariner IV

The Mariner IV spacecraft was launched on 28 November 1964 into an orbit which brought it to the vicinity of Mars on 15 July 1965. A section of the Mariner IV orbit pertinent to this study is shown in Figure 2. The University of Iowa package of particle detectors consists of three end window Geiger-Mueller tubes (EON type 6213) designated A, B, and C and a thin (35 micron) surface barrier solid state detector with two passbands, D_1 and D_2. Table II gives the characteristics of each of the detectors. Each detector has a conical collimator of 60° full angle. The axes of detectors B, C, and D are pointing in the sunward direction at 70° to the spacecraft's roll axis. The axis of detector A makes an angle of 135° with the roll axis looking in the anti-solar hemisphere. The roll axis is maintained to

better than 1° on the sun. Thus, B, C, and D look at particles moving generally away from the sun at angles of 70° ± 30° to the sun-spacecraft line. Similarly, A looks at sunward moving particles at angles of 135° ± 30° to the sun-spacecraft line. The detectors themselves and the inner walls of the collimators are shielded from direct light and x-rays from the sun. The side walls of all detectors have a minimum thickness corresponding to the path length of a ~ 50 MeV proton.

The output of the solid state detector is amplified and clipped to 200 nanoseconds. Two discriminator levels give two proton passbands (Table II). D_1 and D_2 are insensitive to electrons of any energy. To have direct knowledge of the proper operation of this detector in flight, a small $_{95}Am^{241}$ alpha particle source is included to give fixed background counting rates, which have remained identical to their pre-flight values of 0.071 and 0.059 counts/sec. for D_1 and D_2, respectively [Van Allen and Krimigis, 1965].

The Geiger tubes are sensitive to galactic cosmic rays (0.6 c/s), electrons, x-rays, alpha particles, etc. which enter through their collimator and sometimes through their side wall shielding.

The times given for all Mariner IV data herein have been corrected for the propagation time of the signal and are the times that the signals were transmitted. Each detector is sampled once every 6 minutes 43 seconds, except detector B, which is sampled twice in that time interval.

II. OBSERVATIONS

A. Introduction

A summary of the particle observations of Explorer 33 is given in Figure 3. Some selected solar-geophysical data are also included. The crosshatched periods on this and following figures represent the magnetospheric passages of Explorer 33 from shock to shock as seen in Figure 1. These periods are the maximum limits of magnetospheric effects assuming a steady-state magnetospheric configuration. As seen from the figure, during the period under study, two major events took place, the first beginning on 28 January and the second beginning on 13 February with a disturbed period from 1 February to 7 February.

B. The Event of 28 January

As seen by the three Geiger tubes (G1AV, G2, and G3), shown in Figure 4, there were two distinct onsets to this event. Figure 5 shows these two onsets with full available detail (i.e., a resolution of 81.81 seconds) for G1AV. As seen, the first onset of G1AV is at 0215 UT, after which the counting rate rose to a maximum of 8.6 counts/sec. at 0422 UT. The second onset occurred at 0833 UT after which the counting rate rose to a maximum of 698

counts/sec. at 2143 UT. After reaching their maximum intensities, the counting rates of the Geiger tubes decay in an exponential manner with a characteristic time of 1.42 days.

P1 and the other solid state channels all have a very gradual, single increase starting at 0545 UT ± 1 hr. The counting rates then rise to two relative maxima as seen in Figure 6. The first maximum of P1 was at 2214 UT with an intensity of 142 counts/sec. The second maximum of 183 counts/sec. occurred at 1142 UT on 29 January. After the second maximum, the intensity decays with a characteristic time of 1.44 days. By comparison of the four sectors of P1, as shown in Figure 7, one can get some information about the anisotropics of the low energy protons in a plane perpendicular to the ecliptic. For most of the period 28 January through 31 January, the low energy proton flux was isotropic with only a slightly higher counting rate in the sunwards direction indicating a bulk motion of the particles away from the sun (see Figure 7). The one exception to this is the period from about 0000 to 0800 UT which is shown in Figure 8.

The polar cap absorption (PCA) observed by the Douglas 30 mc. riometer at McMurdo, Antartica is shown in Figure 9 with GlAV for comparison. The onset of the PCA is at about 0400 UT 28 January. The absorption then remains at a fairly constant

plateau of 0.5 db from 0445 to 0800 UT, at which time a small decrease occurs. This decrease in absorption may represent an increase in 30 mc. radio noise from the sun rather than a decrease in the absorption. At 0820 UT a sharp increase occurs and by 1700 UT the absorption has risen to 7 db [Masley and Goedeke, 1967].

As shown in Figure 10, the neutron monitors recorded a large increase in intensity on 28 January. The five minute averages of the Deep River neutron monitor for this event are given in Figure 11. As seen in this figure, the onset time was between 0830 and 0835 UT, 28 January.

Figure 2 shows that on 28 January Mariner IV was at a position 82° west of the earth-sun line, and at a distance of 23.85×10^7 km from the sun. Data from the spacecraft are available only for the period 1642 to 2010 UT, 28 January. In Figure 12, these data are presented along with some simultaneous data from Explorer 33 for comparison. The Geiger tubes on Mariner IV all indicate a very high flux of particles (the largest such flux observed by the spacecraft up to that date). Note that the average counting rate of detector B (1.611 counts/sec.) is about a factor of two greater than the counting rate of the other two Geiger tubes, A and C (895 and 820 counts/sec., respectively).

C. The Disturbed Period (from 1 February to 7 February)

At approximately 0000 UT on 1 February all detectors on Explorer 33 show a change in the form of their intensity-time profiles from the exponential decay observed previous to that time. From 1 February through 7 February, the solid state detector exhibits a very complex structure in its intensity-time profiles which has very little correlation with that of the Geiger tubes, as seen in Figure 3. The only readily identifiable feature common to the intensity-time profiles of P3 and G1AV is the peak at 1650 UT on 7 February. The onset times for the increase to this peak are 1340 UT and 1410 UT for G1AV and P3, respectively. G2 and G3 show onsets which are simultaneous with G1AV. The maximum flux measured by G1AV and P3 around 1650 UT are 1814 and 1725 $(cm^2 \text{ sr. sec.})^{-1}$, respectively.

While there is only one simultaneous onset and maximum noted between G1AV and P3, there are four distinct near-simultaneous decreases (actually five, if one counts the decrease from the maximum at 1650 UT, 7 February). These are listed in order in Table III. The gradual decrease at about 0000 UT, 1 February is perhaps another such decrease, although not as abrupt.

During this period from 1 February to 7 February, the disturbed interplanetary conditions are also noted in the neutron monitor readings. Figure 10 shows that there is an enhanced daily variation from 1 February to 7 February. At the same time that the particle detectors indicate that the region has been left behind (or has ceased being disturbed), the variations stop and the neutron monitor readings decend to a minimum. As the neutron monitors recover towards their pre-28 January readings, the particle detectors drop towards their background levels.

D. The Geiger Tube Increase of 2-3 February

At 1909 UT, 2 February a gradual increase was noted on G1AV of Explorer 33. At 0246 UT, 3 February an x-ray flare (evidently caused by the importance 2- flare at 11°N, 58°W, which is listed as starting at 0257 UT) occurred which caused "spill-over" and/or a breakdown of the G1 Geiger tube. "Spill-over" is caused by the reflection of x-rays off of the collimator so that they are seen in sectors II and IV. Also, at times of high counting rates (such as x-ray flares), G1 will give spurious counts caused by a momentary breakdown of the tube. Since it is evident that G1AV has spurious counts

induced during a portion of this event, G2 will be used as the principal detector.

After the onset at 1909 UT, the maximum flux observed by G2 was 172 $(cm^2$ sr. sec.$)^{-1}$ at 2350 UT (Figure 13). During this period, P3 showed no sign of increasing in step with G2. Indeed P2 continued a very gradual decrease which started some two or three hours earlier. At 1001 UT, 3 February a sharp decrease (as previously mentioned) of about a factor of two in a period of six minutes was noted on P2 and the other three solid state chennels. It was also observed on the three Geiger tubes, but with a smaller jump.

In Figure 9, it is seen that at about 2100 UT on 2 February there was the start of a PCA event. This event reached a plateau of 2.5 db at about 0100 UT on 3 February. After 0800 UT, the intensity begins to decay. The sharp dip in the PCA at ~ 0300 UT could be due to radio noise from the flare at 0246 UT previously mentioned. It should be noted that the shape of the absorption curve is well correlated with the intensity-time profile of G2 presented in Figure 13.

The only large flare of importance greater than 1+ that occurred in the four days previous to this event was an importance 2+ flare at 0204 UT on 31 January. The position of this flare

was 28°N, 90°E. In the day preceding the event, only sub-flares of importance 1- were observed. From 1200 to 1510 UT on 2 February, there were several periods of no flare patrol listed in the ESSA, Solar Geophysical Data bulletin of August 1967.

E. The Geiger Tube Increase of 4-5 February

At 1542 UT on 4 February, the Geiger tubes on Explorer 33 record an increase in counting rate. This onset for G1AV, G1X, and P3 is presented in full detail in Figure 14. It is noted that at the onset of G1AV, P3 is at the minimum intensity of a dip that began at 1510 UT. The pre-onset counting rate of G1AV was about 28.2 counts/sec. and immediately following it was 74.3 counts/sec. The pre-onset rate for P3 was 16.5 counts/sec. and following the dip it was 12.4 counts/sec. The entire event is presented in Figure 15. G1AV has not been shown after 0300 UT on 5 February because just after that time the Geiger tube broke down for a short while, making its observations of questionable validity for several hours following. The breakdown was possibly due to the high counting rates encountered from an x-ray event starting at 0012 UT on 5 February. It is also seen from Figure 15 that at 0351 UT on 5 February a near-simultaneous decrease was recorded on both G2 and P3.

F. The 13 February Event

At 1749 UT, 13 February an importance 3 flare occurred at 21°N, 10°W. The optical flare lasted 221 minutes with the maximum phase occurring at 1817 UT. Between 1759 and 1803, a large group of type III radio bursts were reported by the Harvard Radio Astronomy Station at Fort Davis, Texas from 10 to 300 mc. Continuum emissions (14 to 41 mc) was also noted from 1801 to 1829 UT. Explorer 33 registered an x-ray event beginning at 1754 UT (Figure 16). G1AV shows the particle onset at about 1841 UT. The counting rate rose to a maximum of 6.5 counts/sec. at 2117 UT, 13 February. At about 0440 UT, 14 February, the event was obscured as the satellite entered the magnetosphere. After leaving the magnetosphere, Explorer 33 found a strong flux of anisotropic protons. The anisotropy parameters for this period are presented in Figure 17.

G. The Counting Rate Increase of 15-16 February

As shown in Figure 3, all detectors show an increase in particle intensity at 2342 UT on 15 February (Figure 18). At 0848 UT on 16 February there is a sharp decrease in intensity. Simultaneous with the beginning and end of this period of elevated counting rates are two sudden commencements at 2347 UT

on 15 February and 0835 on 16 February, respectively. Also, at about the beginning of this event at approximately 0000 UT on 16 February, a Forbush decrease begins as seen in Figure 10.

From 13 February to 24 February, the intensity-time profile of the alpha particle channel, presented in Figure 6, is very similar to the profiles of the proton channels. In Figure 19, the ratio of channels P2 to P4 is relatively constant and shows this similarity clearly. The one period when this similarity did not hold was during the 16 February increase discussed above. In Figure 20, P2, P4, the ratio of P2 to P4, and the anisotropy parameters for this period are presented in greater detail.

After 0846 UT, 16 February, all detectors show a diminishing particle intensity. By 21 February, GlAV has essentially returned to its background level.

III. RESULTS

A. Onset of 28 January Event

As shown in Figures 10 and 11, very high energy solar protons were present from 0830 UT, 28 January to about 0800 UT, 29 January in sufficient numbers to be detected by neutron monitors. These protons are definitely energetic enough to penetrate the shielding of the detectors on Explorer 33. Thus, it can be stated with confidence that the onset and first peak observed by the solid state detector on all of its channels (see Figure 6) was due to protons penetrating the detector shield. Similarly, the increase noted by the Geiger tubes at 0833 UT can be attributed to these penetrating protons. The particles responsible for the increase observed by the Geiger tubes at 0215 UT cannot be so readily identified. Since P1 showed no increase until about 0545 UT, one can say that the particles in this onset seen by G1AV were not low energy protons. This leaves one with two possible interpretations; that the particles were either protons with $E_p > 10$ MeV or electrons with $E_e > 50$ keV. The fact that the solid state detector does not show an appreciable counting rate during this period, does not rule out the presence of penetrating ($E_p > 60$ MeV) protons since the efficiency of the detector in counting such protons is very low.

The observed polar cap absorption from about 0400 UT to 0800 UT, as seen in Figure 9, could be caused by high energy protons or by relativistic electrons [Masley, private communication]. The possibility of electrons can be eliminated, however, by the increase seen by P1. Since P1 shows a smooth increase beginning at 0545 UT to its maximum, which is known to be caused by protons penetrating its shielding, it is reasonable to assume that the increase at 0545 UT was also due to penetrating protons. Recall also that the solid state detector is insensitive to electrons of any energy. Thus, since P1 indicates that protons are in the vicinity of the spacecraft during this period, one can conclude that both the polar cap absorption and the particles observed by G1AV are protons.

Summarizing these conclusions, one gets the following sequence of events. First, G1AV, which is sensitive to all protons with $E_p > 0.83$ MeV, sees an onset at 0215 UT. At that time, P1 saw nothing above background so the proton energy was above 10 MeV. By about 0400 UT, the flux and/or the energy had increased sufficiently to cause the start of the absorption event, and by 0545 there are enough protons present with $E_p > 60$ MeV for P1 to detect. Then by 0833 UT, the energy and intensity has increased to above the neutron monitor cutoffs and the flux

is rising to the observed intensities of the main portion of the event.

The mechanism responsible for this small flux of energetic protons preceding the main event is uncertain. Several explanations suggest themselves. One is that these particles observed before 0830 UT represent a small leak in a temporary particle storing mechanism somewhere between the earth and the sun. A second possible interpretation is that these protons were actually released from the source flare on the sun before the main injection of energetic particles took place.

From Figure 7, it can be seen that there were significant differences in counting rates between the four sectors of P1, starting at about 0000 UT on 29 January. These differences cannot be explained in terms of a penetrating proton flux because P1 loses its directional sensitivity when particles penetrate its collimator sideways. The particles responsible then must be low energy protons. Figure 8 shows the anisotropy parameters for this period.

B. Particle Identity at Mariner IV

To determine the type of particle observed by Mariner IV, we use the averaged counting rates in Table IV. Note that the counting rates of detectors B and C, which are parallel, differ

by a factor of two, but those of detectors A and C, which look generally sunward and antisunward, respectively, are essentially the same. The latter fact, when considered with the previously mentioned neutron monitor data, would suggest that A and C are counting penetrating protons ($E_p > 50$ Mev). This would mean that roughly half of detector B's counting rate is accounted for by penetrating protons since its omnidirectional characteristics are identical to those of A and C. The difference between B and C then is either due to a very soft flux of electrons ($40 < E_e < 150$ MeV) moving away from the sun, or a flux of low energy protons ($0.5 < E_p < 3.1$ MeV) moving away from the sun. Detector D_1, which is also parallel to B, is sensitive to the low energy protons, but is insensitive to electrons of any energy. Its counting rate, however, is about what one would expect from penetrating protons alone [Krimigis and Van Allen, 1967]. Thus, the interpretation given to the Mariner IV counting rates is as follows. All detectors (A, B, C, D_1, D_2) are counting a large flux of penetrating protons (the largest such flux observed by Mariner IV up to that date). In addition, detector B is counting a large anisotropic flux of low energy electrons.

C. 28 January Flare Location

As stated before, the solar particle event of 28 January had no observed source flare on the visible face of the sun. There was an importance 1- flare starting at 0743 UT, 28 January at position 23°S, 19°E. However, the magnitude of the particle event precludes the possibility that this was the source. In order to find out which areas of the back side of the sun were active at the time of the particle onset, all flares of importance greater than 2- between 1 January and 24 February have been indicated on Figure 21. The position of each flare has been extrapolated back (or forward) to the position at the time of the onset. As seen, there are three groupings of flare-producing regions on the back side. These active areas have been designated areas A, B, and C, where A is located 60° behind the west limb of the sun, B is located 71° behind the east limb of the sun, and C is located 47° behind the east limb. As a point of interest, area A was the region which produced the 13 February flare discussed above. In Figure 2, the regions of the interplanetary magnetic field connected to these active areas have been indicated. The Archimedes spirals have been calculated using solar wind velocities of from 350 to 450 km/sec. The high energy protons will be scattered from these existing field lines by field irregularities [Parker,

1965] but the areas indicated in the figure will have higher particle intensities than elsewhere. The electrons, however, have been found by Lin, Kahler, and Roelof [1967] to be confined to a greater extent than the high energy protons. That is, the diffusion coefficient across the field lines is smaller for electrons than for high energy protons. Thus, one would expect the high energy protons to have a wider angular dispersion than the electrons.

In Table IV, the average values of the detectors of Mariner IV are presented with some simultaneous averages from Explorer 33 for comparison. The flux of penetrating protons observed by Mariner IV was about 70% greater than that observed by Explorer 33, as seen by comparing either detectors A or B with G1AV (the omnidirectional geometric factors for all three detectors are about the same--approximately 0.15 cm^2). Although the omnidirectional geometric factors are not accurately known, the difference would seem to indicate that Mariner IV was closer to the region magnetically connected to the flare.

P2 and P3 are also presented in Table IV. Their counting rates have previously been interpreted as being due to penetrating protons. A direct comparison between P2 and D_1 and P3 with D_2 is not possible due to the low efficiency of the solid state detectors in counting penetrating protons, although their counting

rates are not inconsistent with the presence of comparable intensities of high energy protons present at the position of both spacecraft.

In the previous section, it was shown that a large flux of anisotropic electrons with $E_e \geq 40$ keV were present at the time of the observations. The detectors on Explorer 33 show no comparable flux of electrons. The sun(III) and anti-sun (I) sectors of G1 show a small difference, but this must be attributed to solar x-rays and not to electrons.

The fact that electrons observed at Mariner IV were highly anisotropic would indicate that they had not been diffused to any great extent. This, in turn, implies that Mariner IV is in or very near to the magnetic "tube" connected directly to the flare position on the sun. As seen in Figure 2, either area A or B fits this requirement depending on the solar wind velocity preceding the event. The solar sind velocity at the earth during this period was nearer to 350 km/sec than to 450 km/sec [A. Lazarus, private communication] so area B is considered to be somewhat more probable. The high energy proton data is consistent with this interpretation, although it is inconclusive by itself. All of this discussion, of course, rests on the unsupported assumption that the flare indeed occurred in one of the three active areas.

D. The Diffusive Nature of the 28 January Event

The intensity-time profile of G1AV (Figure 3) from 28 January to 1 February seems to have the shape characteristic of an event propagated by a diffusive mechanism. The fact that this event had no observed source flare, and thus, must have been caused by a flare on the back side of the sun, would also require a diffusive propagation mechanism.

The diffusion model that will be used here is the one proposed by Krimigis [1965]. This is an isotropic diffusion model with a radially dependent diffusion coefficient of the form:

$$D = M\, r^{\beta} \ .$$

The model then requires that the monoenergetic intensity as a function of radius and time have the form:

$$I(r,t) = \frac{Nv}{4\pi(2-\beta)^{(2\alpha+\beta)/(2-\beta)}} \frac{1}{\Gamma[(\alpha+1)/(2-\beta)]} \left(\frac{1}{M}\right)$$

$$\times \frac{1}{t^{(\alpha+1)/(2-\beta)}} \exp\left[-\frac{1}{M} \frac{r^{2-\beta}}{(2-\beta)^2} \frac{1}{t}\right]$$

where $\alpha = 2$ for this case, N is the number of particles injected at $t = 0$, and v is the velocity of a particle of the given energy. From this, it can be shown that a plot of $\ln[I\ t^{(\alpha+1)/(2-\beta)}]$ vs t^{-1} will give a family of straight lines corresponding to the values of β. So to analyze the data by this model, one plots

$$\ln[I\ t^{3/(2-\beta)}] \text{ vs } t^{-1}$$

for various values of β, and determines which value of β gives the best approximation of a straight line. Having determined β in this manner, one gets the diffusion coefficient from the relation

$$D = - \frac{r^2}{(2 - \beta)^2\ m}$$

where m is the slope of the line. From the intercept of the line with the $t = \infty$ axis, one gets N from the relation

$$N = \frac{e^b\ 4\pi(2 - \beta)^{(2\alpha+\beta)/(2-\beta)}\ \Gamma[(\alpha + 1)/(2 - \beta)]\ (M)^{(\alpha+1)/(2-\beta)}}{v}$$

where b is the intercept.

In using this model to analyze the 28 January event, several problems are encountered:

(1) The first is the lack of an observed time for the start of the event. One can make a reasonable approximation by noting that the high energy particles observed to arrive at the onset (about 0830 UT) could not have been injected too much longer than a half hour earlier. Thus, the injection time will be taken to be 0800 UT. Since the early portion of the intensity-time profile is more strongly dependent on the injection time, only data three hours after the presumed start of the event (namely, after 1100 UT) will be used.

(2) The second major problem is due to the fact that the detector being used, GlAV, is sensitive to lower energy protons as well as the higher energies where this model is found to apply best [Krimigis, 1965]. In the latter portion of the event, low energy protons are beginning to reach the vicinity of Explorer 33 and cause higher intensities than one would observe for the high energy protons alone. For this reason, no data later than 15 hours after the presumed start of the event will be used since, by that time, the flux has softened to an extent great enough to effect the results. It should be noted, however, that this upper limit on the usable data of 15 hours may be too high since

it cannot be stated with complete assurance just when the lower energy particles began to arrive in significant numbers. The value found for β, therefore, should be considered a lower limit.

(3) The third problem is what value of energy will best approximate a monoenergetic flux for this event. Since it has been established that the solid state detector was recording particles with sufficient energy to penetrate its sidewall shielding ($E_p > 60$ MeV), we shall take 60 MeV as the equivalent monoenergetic energy. It is noted, however, if this estimate is low by as much as 100 MeV, the value of N will be only a factor of two lower than its true value.

Bearing these difficulties in mind, one sees that a plot of $\ln[I\ t^{3/(2-\beta)}]$ vs t^{-1} (Figure 22) shows that a value of $\beta = 0$ best fits the observed intensity-time profile. By using the slope and intercept of this line and the assumed energy of 60 MeV, one finds the following values:

$$N = 8.8 \times 10^{34} \text{ particles/steradian, and}$$
$$D = 9.8 \times 10^{20} \text{ cm}^2/\text{sec.}$$

From the diffusion coefficient, one can calculate a value for the mean free path λ:

$$\lambda = \frac{3D}{v} = 0.019 \text{ AU}$$

where v is the velocity of a particle of the given energy (60 MeV).

Baird et al. [1967] have analyzed the data from the neutron monitors by this diffusion model. There the data was found to fit a value of $\beta = 1.1$ best, and yielded a value of the diffusion coefficient D of about 7×10^{21} cm^2/sec. For an energy of ~ 450 MeV (about the cutoff energy of the Deep River neutron monitor) this indicates a mean free path of ~ 0.061 AU.

The difference in β between the two results is not unreasonable. It was shown by Krimigis [1965] that for a given event, β as a function of energy tended to increase rapidly from low values at energies below $\sim$ 50 MeV and then tended to flatten out at higher energies to a constant value of about 1.0. These results seem to agree favorably with energy dependence of β when one recalls that the value of $\beta = 0$ is to be considered a lower limit.

A comparison of the two values of the mean free path gives some information about the scale size distribution of the interplanetary magnetic field irregularities. The value of λ for lower energies ($\lambda \cong 0.02$ AU for $E_p \cong 60$ MeV) compared to that of higher energies ($\lambda = 0.06$ AU for $E_p \cong 450$ MeV) indicates that there are relatively more irregularities of a size comparable

to the gyro-radius of a 60 MeV proton (~ 0.002 AU) than to the gyro-radius of a 450 MeV proton (~ 0.006 AU) since the most effective size scattering center is one comparable to the gyro-radius of the particle [Parker, 1964]. This result agrees with the observations of Coleman [1966].

E. The Disturbed Period (from 1 February through 7 February)

After the decay phase of the 28 January event ended at about 0000 UT on 1 February, the form of the intensity-time profiles of the Explorer 33 detectors become quite complex. During this disturbed period, the particle fluxes recorded by the solid state detector and the Geiger tubes had essentially no correlation with each other, as seen in Figure 3. It is recalled that both detectors are sensitive to low energy protons $E_p < 10$ MeV, while the Geiger tubes are also sensitive to protons with $E_p > 10$ MeV. We will assume, for the present, that electrons make significant contributions to the counting rates of the Geiger tubes only for relatively short times and will be ignored here. This indicates that the fluxes of the low energy and the high energy protons are essentially independent. This is interpreted to mean that the interplanetary magnetic field has modulated the original spectrum of the particles since this

type of spectrum is typical only of the early portions of solar particle events [Armstrong, Krimigis, and Van Allen, 1967]. Thus, it can be said that the particles present during this period were not recently generated by a flare or combination of flares, but had been semi-trapped in the interplanetary magnetic field for some time. The complex intensity-time profile of this period also supports this view.

The only points of similarity between the intensity-time profiles of the solid state detector and the Geiger tubes were found to be the decreases listed in Table IV, the maximum at 1650 UT on 7 February. Since at that time, P3 and G1AV both observed about the same flux (1725 and 1814 $(cm^2 \text{ sr. sec.})^{-1}$, respectively), it can be said that there was only a small flux of protons with $E_p > 1.9$ MeV present.

During the disturbed period, the neutron monitors recorded an enhanced daily variation. The maximum of this variation occurred at about 0000 UT every day for the neutron monitors shown in Figure 10. Since the period of enhanced daily variations begins and ends at the same time as the disturbed period, as shown by the Explorer 33 particle detectors, it can be concluded that the magnetic configuration modulating the lower energy particles fluxes are also modulating the glactic cosmic ray fluxes observed by the neutron monitors.

If the decreases noted in Table III mark the co-rotating sector boundaries [Wilcox and Ness, 1965], it is easily shown that the characteristic width of these sectors at the orbit of the earth is about 5×10^7 km. For a 4 gamma field, this corresponds to a gyro-radius of a 60 BeV glactic cosmic ray proton. This is seen to be well above the neutron monitor cutoffs shown in Figure 10. Thus, it is clear that the field structures of the disturbed period are easily large enough to cause a strong modulation of the glactic cosmic ray flux as observed.

F. The Presence of Protons with $E_p > 10$ MeV During the Disturbed Period

At 1909 UT on 2 February, G2 recorded a gradual increase in counting rate. As seen in Figure 13, P3 does not show a corresponding increase. From this fact, and the fact that none of the other solid state channels recorded an increase like that observed by G2 (see Figure 6), it is seen that protons of energy less than 10 MeV were not responsible for the increase. Thus, the particles causing this increase in G2 were either protons with $E_p > 10$ MeV or electrons with $E_e > 45$ keV.

In Figure 9, it is seen that there is a polar cap absorption event starting at about 2100 UT on 2 February, which reaches

a maximum of about 2.5 db by 0100 UT on 3 February. Assuming the particles to be a monoenergetic flux of 10 MeV protons, we find that the observed difference in flux between P3 and G2 is sufficient to cause an absorption of ~ 3 db [Adams and Masley, 1965]. Thus, the particles responsible for the G2 increase and the PCA are probably protons with $E_p > 10$ MeV.

There are two possible sources of these high energy protons that would give the observed type of onset: (A) semi-trapped protons that were emitted from a large flare up to several days previous to the observation and were confined to a "tube" of magnetic field lines that connect directly to the flare position on the sun or (B) prompt protons from a flare that had occurred within the previous several hours.

Case A: The only large flare of importance greater than 1+ in the four days preceding this event was the 2+ flare occurring at 0204 UT on 31 January (see Figure 3). This flare was located at 28°N, 90°E. At the onset of the event, solar rotation would have brought this area to about 58°E. Assuming a solar wind velocity between 300 and 500 km/sec., it is seen that the field lines in the vicinity of the earth originate from 61° ± 15°W on the sun. So semi-trapped particles are not responsible for the increase recorded by G2.

Case B: The only flares in the period immediately preceding the event were sub-flares of importance 1-. It seems very unlikely that any of these could have caused an appreciable high energy proton event.

This leaves two possible interpretations: that a large flare occurred during one of the periods of no flare patrol mentioned previously, or that the event was caused by a flare occurring on the back side of the sun. From the available data, it is not possible to say which of these was the case.

G. The Presence of Electrons During the Disturbed Period

At 1542 UT on 4 February, GlAV observed an increase in counting rate (Figure 14) from 28 to 74 counts/sec. This indicates that the particles causing this increase were either protons with $E_p > 0.83$ MeV or electrons with $E_e \geq 50$ keV. The onset observed by GlAV occurred at the minimum intensity of a dip in the counting rate reported by P3. Before the onset of this event, P3 was indicating a larger flux of low energy protons than was observed later. In Figure 6, it is seen that the intensity-time profile of P1 and P2 are similar in form to that of P3 for this period. The drop in counting rates of all of the solid state detector channels after the dip indicates that the population of protons with $0.31 \leq E_p \leq$

10 MeV has decreased in the vicinity of Explorer 33. Thus, it is seen that the particles causing the onset of G1AV were either protons of $E_p > 10$ MeV or electrons with $E_e > 50$ keV.

In Figure 9, it is seen that there was no increase in PCA that can be correlated with the particle onset. The increase in flux observed would give an absorption of ~ 2 db, assuming the particles were a monoenergetic beam of protons with $E_p = 10$ MeV. Thus, it can be concluded that the particles observed by G1AV and the other Geiger tubes were electrons with $E_e > 45$ keV.

The intensity-time profile of this event (Figure 15) is very similar to the delayed electron event observed by Lin and Anderson [1967] for the 29 August 1966 event, in that it has both a fast onset and a sharp decrease. This profile is very atypical of prompt electron events, which have a more gradual decrease. The profile of P3 also indicates that this was not a prompt electron event. The coincidence of the arrival of prompt electrons and the arrival of an intensity dip being propagated with low energy protons at a much lower velocity than that of the electrons, would seem very unlikely.

On the basis of the foregoing, it it concluded that the electrons observed in this event were trapped in a region of the interplanetary magnetic field whose two boundaries are marked by the dip in the low energy proton intensity and the onset of the

electrons, and by the sudden decrease noted in all detectors at 0215 UT on 5 February. The width of this region as measured along the orbit of the earth was about 1.5×10^7 km.

The only large flare for a few days preceding this event was the importance 2- flare observed at 0257 UT on 3 February at 11°N, 58°E. By the time of the onset solar rotation would have carried the flare only to 37°E. Since the field lines in the vicinity of the earth are connected to the sun at about 61° ± 15°W, it is seen that this flare was not responsible for the event. Lin and Anderson [1967] have reported that flares with importance as small as 1- have been observed to produce electrons so presumably one of these could have injected the electrons into the trapping region. In view of the number of sub-flares during this period, a search for the particular flare responsible for this event would prove hopeless, and will not be attempted.

H. The 13 February Event

At 1749 UT on 13 February, an importance 3 flare accompanied by a large x-ray event caused a particle increase beginning at 1841 UT (see Figure 16). At about 0440 UT on 14 February, the event was obscured as Explorer entered the magnetosphere. Upon emerging, the large anisotropy noted by P1 indicates a large flux

of low energy protons flowing outward from the sun as seen in Figure 16. The flux at 1550 UT, 15 February for G1AV and P3, respectively are 193.2 and 311.1 $(cm^2$ sr. sec.$)^{-1}$. Since P3 and G1AV have the same threshold energy, one would expect that the latter would always measure the greater flux of the two detectors if it is a valid approximation of a spin-averaged detector. To check this, one examines the proton flux for anisotropies in sector III of P1. In Figure 7, we see that sectors II and III of P1 have elevated intensities at this time compared to sectors I and IV. Thus, a large portion of the flux of protons is incident on G1 in sector III, which is excluded in the calculation of G1AV. This means that G1AV is counting at a rate which is considerably lower than true omnidirectional detector would give.

At about 0000 UT on 16 February, a Forbush decrease occurred as seen in Figure 10. It has been suggested by other workers [Rao, McCracken, and Bukata, 1967] that there is a period with a bi-directional anisotropy following the decreasing phase of the Forbush decrease. That is, an anisotropy with two maxima in the angular distribution aligned parallel and antiparallel to the interplanetary magnetic field. Assuming that the magnetic field was approximately at the prevailing garden hose angle, the two peaks should appear in sectors I and III of P1 (see the spin

vector in Figure 1). A search of the separate sectors of P1 (Figure 7) reveals no such period between 0000 UT, 16 February and 0000 UT, 24 February. In fact, whenever any anisotropy is present at all, sector I invariably had the lowest counting rate. Assuming the anisotropy had the form

$$P1(\theta) = A[1 + C \cos(\theta + \delta)]$$

as before, the values of δ and C are presented in Figure 20 for the period around the Forbush decrease.

I. The Counting Rate Increase of 15-16 February

At 2342 UT on 15 February, all detectors showed an increase of what is interpreted to be a flux of low energy protons. Only small sub-flares of importance 1 or 1- had occurred for the previous two days so these are not particles from a flare just arriving at the earth (see Figure 16). The last large flare was the one discussed above that occurred on 13 February at 10°W longitude. At 0000 UT on 16 February, the region which produced this flare had been rotated to about 40°W. If we assume that the interplanetary magnetic field lines in the vicinity of the earth originate at this position, then we obtain plasma velocities

of 700 ± 50 km/sec. corresponding to the observed increase. This is somewhat higher than the usually observed values of 350-450 km/sec., but is not unreasonable. At 0848 UT on 16 February, all detectors show a sharp decrease in particle fluxes.

At the beginning and end of the period of enhanced intensities shown in the figure, two sudden commencements were noted on the earth. A somewhat similar case of sudden commencements occurring on both ends of a sharp spike of particle intensity was noted by Lin and Anderson [1967] in the 29 August 1966 event.

J. Low Energy Proton Spectrum

Using the nested energy ranges of P1, P2, and P3 (Table I) one can make some statements about the differential energy spectrum of the low energy protons. The ratio of any two of the channels has two corresponding spectral slopes, one rising with energy and the other falling. Using all three ratios, ideally one should be able to select one or the other. However, in the case of the rising spectrum, the knowledge of the exact value of the upper limit of the energy range becomes critical. Since this limit is not known with accuracy, the interpretation of a rising spectrum is unclear [Armstrong, Krimigis, and Van Allen, 1967].

Plotted in Figure 23 are P1, the three ratios, and the spectral parameter E_o for a falling differential spectrum of the form:

$$\frac{dj}{dE} = \frac{N}{E_o} e^{-\frac{E}{E_o}} ,$$

the values plotted are one hour averages taken every quarter day. As seen, the agreement of the E_o's derived from the different ratios are at times poor and at times the ratios cannot be fitted to the model spectrum at all.

From 0800 UT, 28 January until about 0800 UT, 29 January, it is known that there are penetrating protons present so that the ratios are not a valid measure of the low energy proton spectrum. From 0200 until 1200 UT on 29 January, the low energy proton spectral slope is interpreted to be rising with energy. This interpretation is based on the relative shapes of the counting rate contours of the Geiger tubes and the solid state channels (Figure 3) . The Geiger tubes show an intensity generally decreasing in time, while the solid state detector shows the intensity increasing until about 1200 UT, 29 January. Thus, the slope is becoming less and less rising until at 1200 UT it begins

to fall. From 1200 UT, 29 January to 0000 UT, 1 February, the ratios are valid and generally constant indicating an E_o of about 470 keV.

After the magnetospheric passage on 1-2 February, the ratios again become generally constant indicating an E_o of about 500 keV. On 7 February, there is a decrease in all ratios until about 0600 UT, 8 February the E_o is about 250 keV. The spectral parameter remains low for the period 8 to 11 February with a value of about 350 keV. From 11 February to about 1800 UT, 13 February, the counting rates are too low for the ratios to be reliable.

At about 1800 UT, 13 February, just before the second magnetospheric passage, the spectrum again evidently becomes a rising one for reasons similar to those outlined about. After the magnetospheric passage, the spectral parameter is reasonably constant with a value of about 400 keV. The ratios become statistically unreliable after 21 February.

Summarizing the spectral information, the low energy proton spectrum divides the period of interest up into four main parts:

(1) 1200 UT, 29 January to 0000 UT, 1 February; decay of intensity from 28 January flare; $E_o \sim 500$ keV.

(2) 0000 UT, 4 February to 0000 UT, 7 February; disturbed period; $E_o \sim 470$ keV.

(3) 0000 UT, 8 February to 0000 UT, 11 February; decay from disturbed period; $E_o \sim 350$ keV.

(4) 1800 UT, 13 February to 0000 UT, 21 February; decay from 13 February flare; $E_o \sim 400$ keV.

K. Alpha Particles and the Proton to Alpha Particle Ratio

In Figure 6, the counting rate of the alpha particle channel (P4) of the solid state detector is shown in comparison to the three other channels of that detector. The intensity-time profile of the proton channels are very similar to that of the alpha particle channel, suggesting that the ratio of protons to alpha particles is relatively constant, even over variations in intensity of several orders of magnitude.

The relative number of protons to alpha particles can be inferred from the ratio of channels P2 to P4. The pass bands of the two channels are very similar when expressed in energy per nucleon, where P2 is $0.50 \leq E_p \leq 4.0$ MeV/nucleon and P4 is $0.52 \leq E_\alpha \leq 4.2$ MeV/nucleon. This difference is small and will be ignored for this discussion. The validity of this ratio is

dependent on whether alpha particles are making a significant contribution to the counting rate of P2, and whether alpha particles are the only constituent of the counting rate of P4. The only significant source of spurious counts in P4 that needs to be considered here is that of penetrating protons [Armstrong, Krimigis, and Van Allen, 1967; Krimigis and Van Allen, 1967]. Penetrating protons are known to be present from 0800 UT, 28 January, but are not known to be present in significant numbers at other times.

If one assumes that the spectral parameter E_o for the alpha particles is the same as for protons when expressed in MeV/nucleon [Armstrong, Krimigis, and Van Allen, 1967] then it is easily demonstrated that for the spectra and the counting rates observed during the period of interest, the maximum contribution that alpha particles could make to the counting rate of P2 is 5%. Thus, P2/P4 can be considered a reasonably valid ratio of the abundance of protons to alpha particles except for the period 0800 UT, 28 January to 0800 UT, 29 January when penetrating protons are present.

This ratio is presented in Figure 19 (3-hour averages) with the counting rate of P2. Between 29 January and 5 February the ratio shows a slow but steady decline from 60 to 30. The stability of this ratio is surprising is view of the wide range

of intensities and in comparison with the variations in the proton to alpha particle ratio reported by other workers [Armstrong, Krimigis, and Van Allen, 1967]. From 6 to 9 February there is an increase in the ratio indicating the presence of relatively more protons as one approaches the time of the low energy proton peak on 7 February, previously mentioned. From 11 February through 13 February, the ratio is statistically unreliable.

Just before entering the magnetosphere, the ratio jumps to a peak of almost 200 indicating that there was a large excess of protons immediately after the onset of the flare. After the magnetospheric passage, the ratio remains on a fairly constant plateau of 60 to 70 until the rt becomes statistically unreliable after 20 February.

The one major deviation from this plateau is noted on 16 February just as the "core" of the 13 February flare sweeps past the earth. The half hour averages of the ratio and other data have been plotted in Figure 20. The graphs of P2 and P4 clearly show that it was an excess of protons in the first part of the core rather than a lack of alpha particles that caused the spike in the ratio. In the second half of the core, the ratio was about the same as the following plateau. This is the first reported observation of such a variation in the proton to alpha particle ratio.

During the passage of the core there were significant but generally weak anisotropies in the low energy proton flux. As seen from the figure, there is a period of anisotropy generally from the north, which begins about two hours before the core arrives and ends about two hours before it passes. Without magnetometer data, it is unclear what interpretation to give this. It is interesting to note, however, that the proton to alpha spike it almost exactly centered in this region.

Several possible explanations for this phenomenon suggest themselves. If there is no diffusion across the magnetic field then this might be a "map" of the proton to alpha particle ratio on the sun, allowing for the intertwining of the field lines. If one postulates a diffusive process and assumes a constant proton to alpha particle ratio at the sun then the observed spike is evidently due to a difference in the diffusion constant of the alpha particles and protons for different tubes of magnetic field. Since an alpha particle has twice the rigidity of a proton of the same energy per nucleon, a rigidity dependent scattering mechanism would seem to be indicated. If this is the case then this ratio would be a significant probe of the interplanetary field irregularities. Midway between these two cases is a combination, that is, diffusion near the sun but none further out. One way

of deciding between these possibilities would be to make observations of this phenomenon simultaneously at several radial distances. The complete explanation of this effect awaits further study.

IV. SUMMARY OF RESULTS

(1) Preceding the main onset of the 28 January event at 0833 UT, there was a small flux of high energy protons ($E_p > 10$ MeV) beginning at 0215 UT whose spectrum gradually hardened until the solid state detector observed them as penetrating protons ($E_p > 60$ MeV) at 0545 UT.

(2) Mariner IV, located 82° west of the earth-sun line, 23.85×10^7 km from the sun, during the period of available data from 1642 to 2010 UT on 28 January observed large fluxes of highly anisotropic electrons ($E_e > 40$ keV) and penetrating protons ($E_p > 55$ MeV). This proton flux was larger than that observed by comparable detectors on Explorer 33. No electrons were observed at Explorer 33.

(3) It was observed that the 28 January event had no source flare on the visible face of the sun. At that time there were three active areas on the back side of the sun. If the flare is assumed to have come from one of these areas, it was found by comparison of the particle fluxes observed by Mariner IV and Explorer 33 that the most probable of the three was located 71° behind the east limb of the sun.

(4) It was found that the first portion of the 28 January event consisting of protons with $E_p > 60$ MeV could adequately

described by an isotropic diffusion model [Krimigis, 1965]. From the diffusion constant found by use of this model, a value of the mean free path λ was calculated to be approximately 0.019 AU. A comparison of this with the results of a similar analysis of the neutron monitor increase by Baird et al. [1967] indicated that there were relatively more interplanetary magnetic field irregularities with a scale size of ~ 0.002 AU than with a scale size of ~ 0.006 AU.

(5) The disturbed period from 1 February through 7 February was found to be populated with particles whose energy spectrum had been strongly modulated by the interplanetary magnetic field. Sudden decreases in the counting rates of all detectors indicated at least four possible sector boundaries. The scale size of these regions, best indicated by the strong variations in the low energy proton population, was found to be sufficient to produce the enhanced daily variations observed in the neutron monitor during this period.

(6) At 1090 UT on 2 February the onset of a flux of high energy protons ($E_p > 10$ MeV) was observed. No adequate source flare for this event could be located. It was concluded that either a large flare had occurred during an earlier period of no flare patrol, or that the source flare was located on the back side of the sun.

(7) From 1545 UT on 4 February to 0215 on 5 February, a flux of electrons contained in a magnetic field configuration 1.5×10^7 km wide at the earth's orbit was observed. The source of these electrons could not be determined.

(8) At 1841 on 13 February, the onset of a particle event caused by an importance 3 flare at 1749 UT was observed. By 2342 UT, 15 February when a period of increased particle intensity started, the region producing this flare had been moved to 40°W by the rotation of the sun. This would indicate a solar wind velocity of 700 ± 50 km/sec., which is higher than the usually observed 350 to 450 km/sec. but is not considered unreasonable.

(9) Using the solid state detector, a value can be obtained for the spectral parameter E_o of a falling exponential differential spectrum for the low energy protons. During the period under study, it was found that the period when E_o was valid could be divided into four sections:

(a) 1200 UT, 29 January to 0000, 1 February; decay of intensity from 28 January flare; $E_o \sim 500$ keV.

(b) 0000 UT, 4 February to 0000 UT, 7 February; disturbed period; $E_o \sim 470$ keV.

(c) 0000 UT, 8 February to 0000 UT, 11 February; decay from disturbed period; $E_o \sim 350$ keV.

(d) 1800 UT, 13 February to 0000 UT, 21 February; decay from 13 February flare; $E_o \sim 400$ keV.

(10) The proton to alpha particle for particle of the same energy per nucleon (from 0.5 to 4.0 MeV/nucleon) was found to be remarkably constant considering the variations in intensities observed. The one interesting deviation from this is summarized below.

(11) During the period of increased particle intensities from 2342 UT on 15 February to 0848 UT on 16 February there were two maxima in both proton and alpha particle intensities. During the first peak relative excess of protons was noted in comparison to the second peak and the period following 0848 UT. The value of the proton to alpha particle ratio for the two peaks are ~ 165 and ~ 60, respectively. This is the first reported observation of such a variation in this ratio.

TABLE I

Principal Characteristics of Explorer 33 Detectors***

Detector	Thresholds for Detectable Radiation	COLLIMATOR Full Angle	COLLIMATOR Axis Direction	Reciprocal Geometric Factor
P1	$0.31 \leq E_p \leq 10$ MeV** $0.59 \leq E_\alpha^p \leq 225$ MeV**	Conical, 60°	$\perp$ to spin axis, sectored	12.2 $(cm^2\ sr)^{-1}$
P2	$0.50 \leq E_p \leq 4.0$ MeV** $0.78 \leq E_\alpha^p \leq 98$ MeV**	"	$\perp$ to spin axis	"
P3	$0.82 \leq E_p \leq 1.9$ MeV** $1.13 \leq E_\alpha^p \leq 46$ MeV**	"	"	"
P4	$2.1 \leq E_\alpha \leq 17$ MeV**	"	"	"
GM1	$E_e \gtrsim 50$ keV* $E_p \gtrsim 830$ keV	Fan, 30° equatorial 90° meridian	$\perp$ to spin axis, sectored	28 $(cm^2\ sr)^{-1}$
GM2	$E_e \gtrsim 45$ keV* $E_p \gtrsim 730$ keV	Conical, 40°	parallel to spin axis	50 $(cm^2\ sr)^{-1}$
GM3	$E_e \gtrsim 45$ keV* $E_p \gtrsim 730$ keV	Conical, 40°	anti-parallel to spin axis	42 $(cm^2\ sr)^{-1}$

*GM tubes also sensitive to x-rays ~ 2 to 12 Å.

**Upper thresholds are accurate to ± 10%.

***After Armstrong, Krimigis, and Van Allen [1967].

TABLE II

Mariner IV Detectors*

Detector	Unidirectional Geometric Factor (cm^2 sr)	Omnidirectional Geometric Factor (cm^2)	Particles to Which Sensitive
A	0.044 ± 0.005	~ 0.15	Electrons: $E_e \gtrsim$ 45 keV Protons: $E_p \gtrsim$ 670 ± 30 keV
B	0.055 ± 0.005	~ 0.15	Electrons: $E_e \gtrsim$ 40 keV Protons: $E_p \gtrsim$ 550 ± 20 keV
C	0.050 ± 0.005	~ 0.15	Electrons: $E_e \gtrsim$ 150 keV Protons: $E_p \gtrsim$ 3.1 MeV
D_1	0.065 ± 0.003	--	Electrons: none Protons: $0.50 \leq E_p \leq 11$ MeV
D_2	0.065 ± 0.003	--	Electrons: none Protons: $0.88 \leq E_p \leq 4.0$ MeV

*After Van Allen and Krimigis [1965]

TABLE III

Sudden Decreases

1 February to 9 February

Date	G1AV Decrease Time	P1 Decrease Time
3 February	1001	1001
5 February	0257	0251
6 February	1329	1353
8 February	1240	1306

TABLE IV

Counting Rate Averages of Explorer 33
and Mariner IV for 1642 to 2010 UT, 28 January

Explorer 33	Mariner IV
G1 (Sector I) = 560 counts/sec	A = 895 counts/sec
G1 (Sector III) = 676 counts/sec	B = 1,611 counts/sec
G1AV = 578 counts/sec	C = 820 counts/sec
P_2 = 41 counts/sec	D_1 = 41 counts/sec
P_3 = 18 counts/sec	D_2 = 15 counts/sec

REFERENCES

Adams, G. W. and A. J. Masley, "Theoretical study of cosmic noise absorption due to solar cosmic radiation," Douglas Aircraft Company Paper No. 3112 (1965).

Armstrong, T. P., S. M. Krimigis, and J. A. Van Allen, "Observations of the solar particle event of 7 July 1966 with University of Iowa detectors," Proc. COSPAR Symposium, London (1967).

Baird, G. A., G. G. Bell, S. P. Duggal, and M. A. Pomerantz, "Neutron monitor observations of high energy solar particles during the new cycle," Bartol Research Foundation Research Report (1967).

Coleman, P. J., "Variations in the interplanetary magnetic field: Mariner II," J. Geophys. Res. 71, 5509-5531 (1966).

Krimigis, S. M., "Interplanetary diffusion model for the time behavior of intensity in a solar cosmic ray event," J. Geophys. Res. 69, 2943-2959 (1965).

Krimigis, S. M. and J. A. Van Allen, "Geomagnetically trapped alpha particles," J. Geophys. Res. 72, 5779-5797 (1967).

Lin, R. P. and K. A. Anderson, "Electrons > 40 keV and protons > 500 keV of solar origin," Solar Phys. 1, 446-464 (1967).

Lin, R. P., S. W. Kahler, and E. C. Roelof, "Solar flare injection and propagation of low energy protons and electrons of the event of 7-9 July 1966," Proc. COSPAR Symposium, London (1967).

Masley, A. J. and A. D. Goedeke, "The 1966-1967 increase in solar cosmic ray activity," presented at the Tenth International Conference on Cosmic Rays, Calgary, Canada (1967).

Parker, E. N., "The scattering of charged particles by magnetic irregularities," J. Geophys. Res. 69, 1755-1758 (1964).

Parker, E. N., "The passage of energetic charged particles through interplanetary space," Planet. Space Sci. 13, 9-49 (1965).

Rao, U. R., K. G. McCracken, and R. P. Bukata, "Cosmic ray propagation processes. 2. The energetic storm particle event," J. Geophys. Res. 72, 4325-4341 (1967).

Van Allen, J. A. and S. M. Krimigis, "Impulsive emission of ~ 40 keV electrons from the sun," J. Geophys. Res. 70, 5747-5751 (1965).

Wilcox, J. M. and N. F. Ness, "Quasi-stationary corotating structures in the interplanetary medium," J. Geophys. Res. 70, 5793-5805 (1965).

Figure 1 The eliptic plane projection of the Explorer 33 orbit in solar ecliptic coordinates. The projection of the spin vector has been included at intervals. The spin vector is inclined about 5° north of the ecliptic plane.

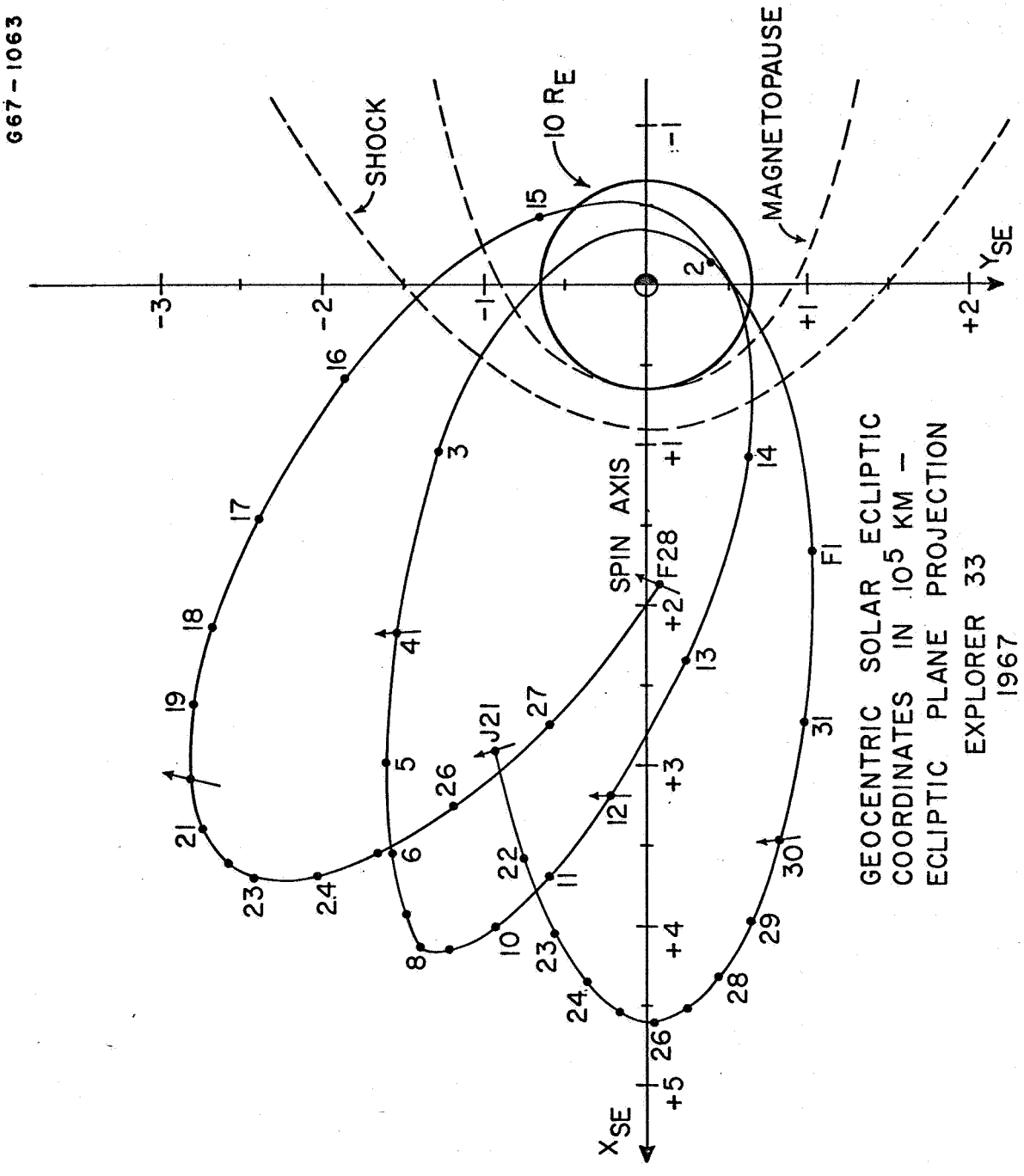
G67-1063
SHOCK
10 R_E
MAGNETOPAUSE
Y_{SE}
X_{SE}
SPIN AXIS
GEOCENTRIC SOLAR ECLIPTIC
COORDINATES IN 10^5 KM -
ECLIPTIC PLANE PROJECTION
EXPLORER 33
1967

Figure 1

Figure 2 A portion of the Mariner IV trajectory from December 1966 to March 1967. The coordinate system holds the earth-sun line fixed. The three back side active regions and their "garden hose regions" are indicated (see text).

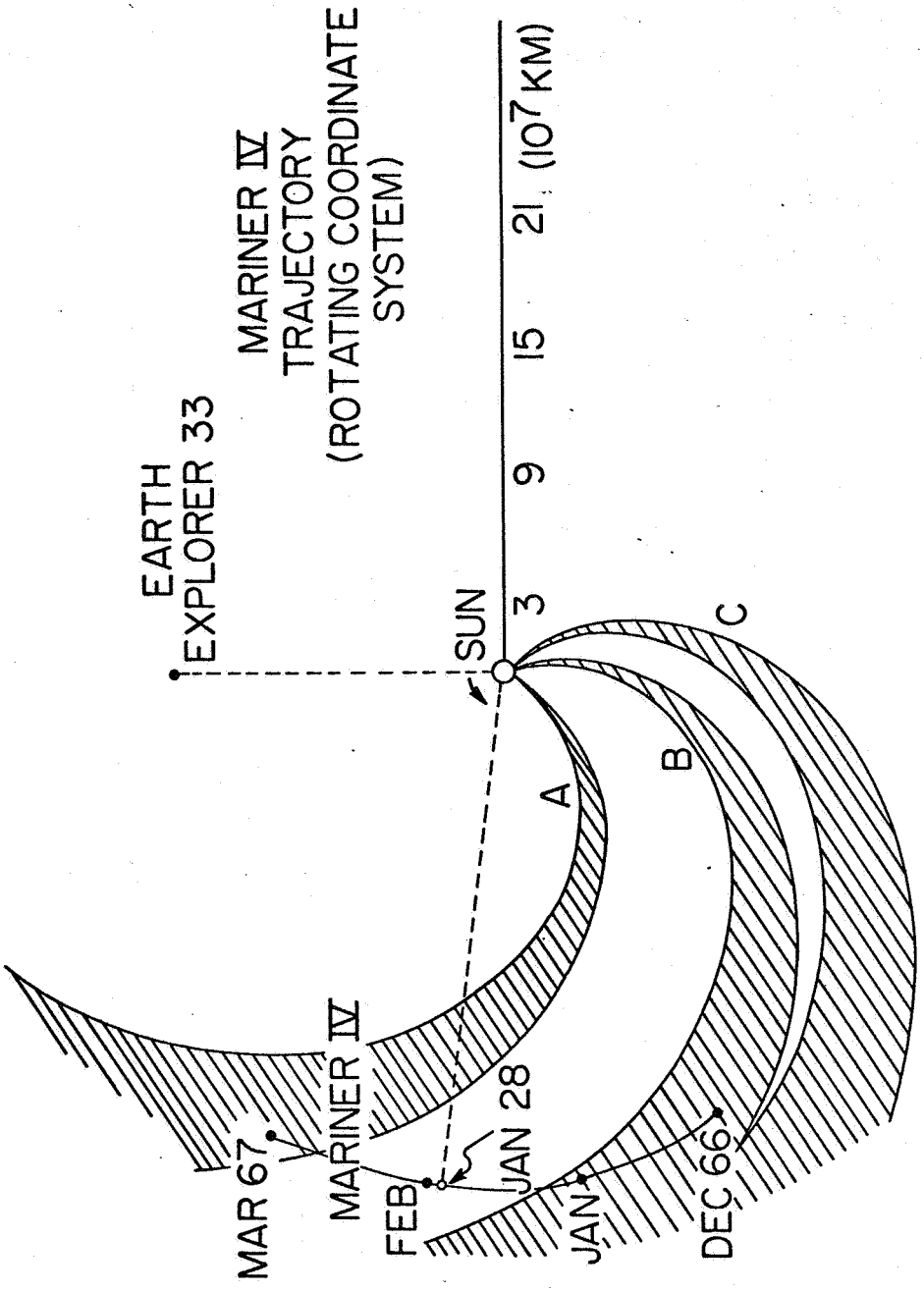
G67-1076
MARINER IV
TRAJECTORY
(ROTATING COORDINATE
SYSTEM)
EARTH
EXPLORER 33
SUN
3
9
15
21 (10⁷ KM)
A
B
C
MAR 67
MARINER IV
FEB
JAN 28
JAN
DEC 66

Figure 2

Figure 3 A summary of the Explorer 33 observations. The one-hour averages of P3 and G1AV are presented. Note that these detectors have the same threshold for protons (Ep = 0.83 MeV). Some solar-geophysical data have been included. The crosshatched regions are magnetospheric passages from shock to shock.

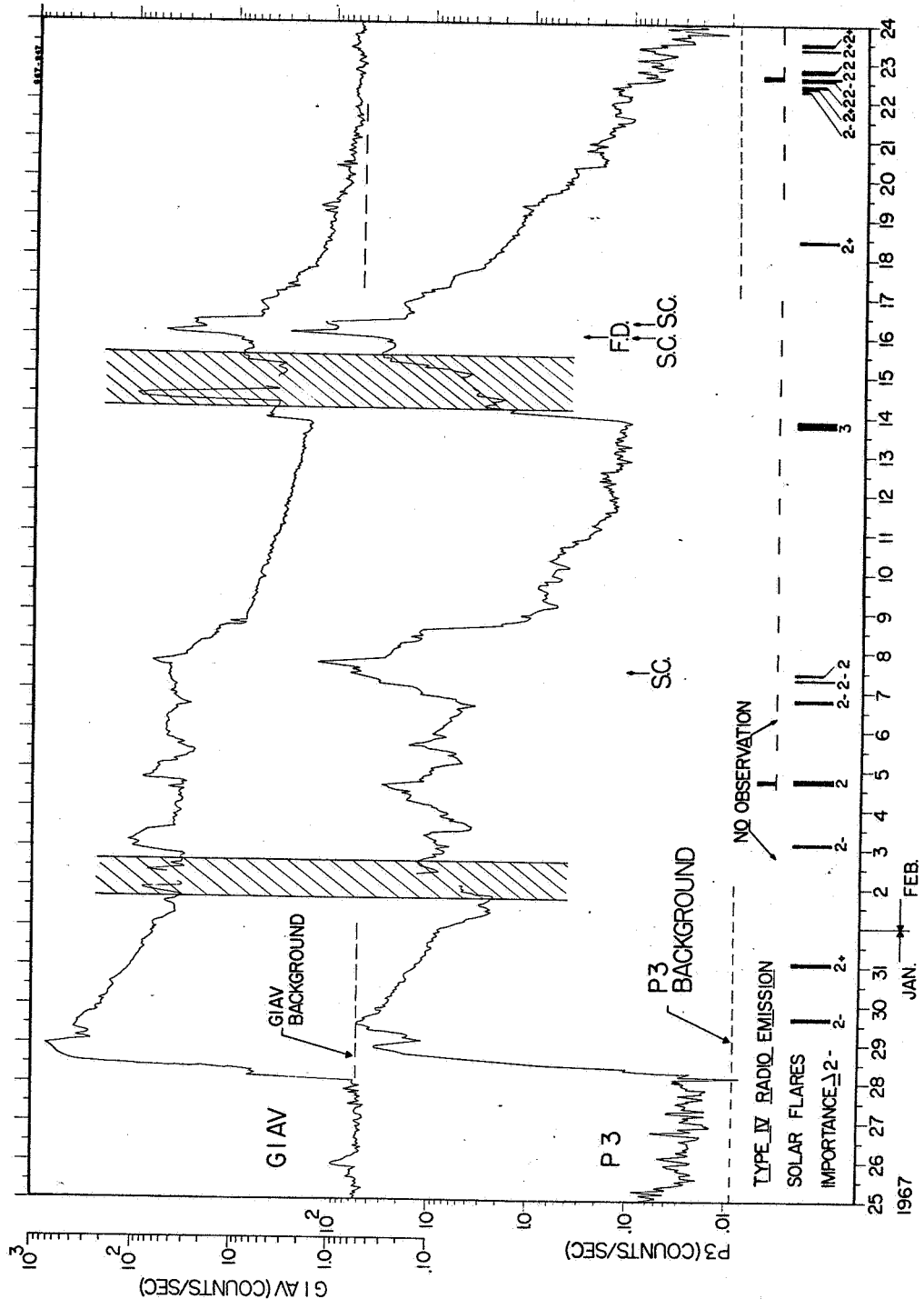
G1AV (COUNTS/SEC)
P3 (COUNTS/SEC)
G1AV
G1AV BACKGROUND
P3
P3 BACKGROUND
NO OBSERVATION
TYPE IV RADIO EMISSION
SOLAR FLARES
IMPORTANCE ≥ 2-
F.D.
S.C.
S.C.
S.C.
JAN.
FEB.
1967

Figure 3

Figure 4 G1AV, G2, and G3 one-hour averages. The crosshatched regions are magnetospheric passages from shock to shock.

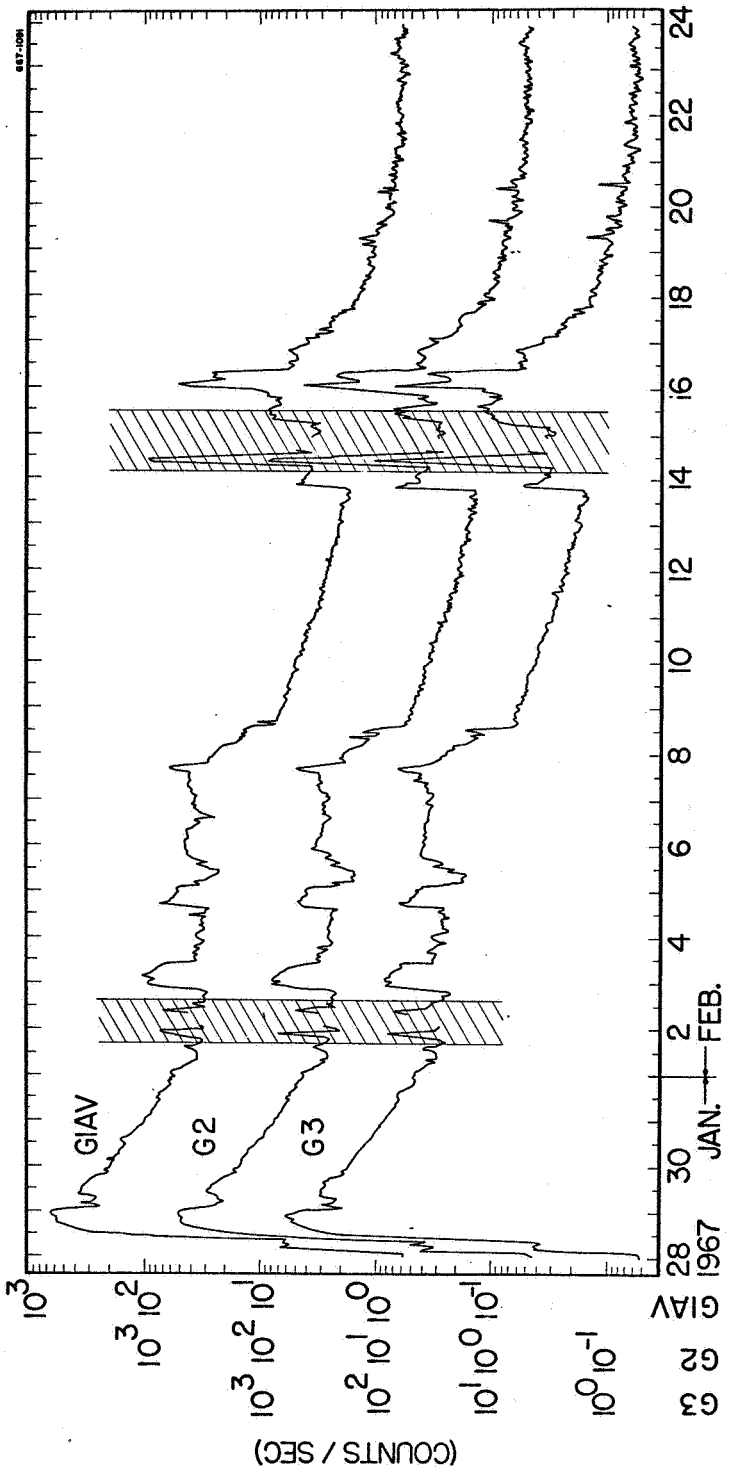
GIAV
G2
G3
28
30
JAN.
2
FEB.
1967
4
6
8
10
12
14
16
18
20
22
24
10^3
$10^3\,10^2$
$10^3\,10^2\,10^1$
$10^2\,10^1\,10^0$
$10^1\,10^0\,10^{-1}$
$10^0\,10^{-1}$
GIAV
G2
G3
(COUNTS / SEC)

Figure 4

Figure 5 Full detail plot of the 28 January onsets for GlAV.

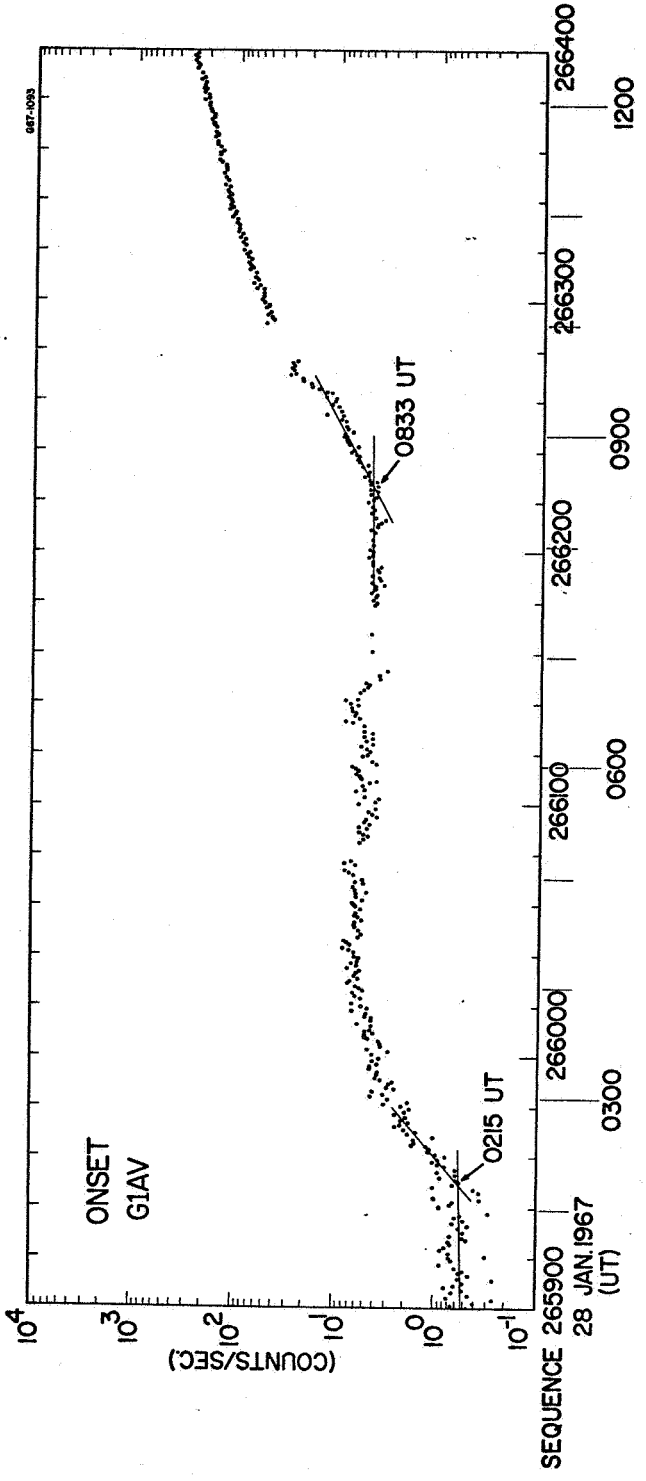
687-1093
ONSET
G1AV
0833 UT
0215 UT
(COUNTS/SEC.)
10^4
10^3
10^2
10^1
10^0
10^{-1}
SEQUENCE 265900
28 JAN.1967
(UT)
0300
266000
0600
266100
0900
266200
1200
266300
266400

Figure 5

Figure 6 One-hour averages of the four solid state detector channels. P4 counts alpha particles only. The cross-hatched regions are magnetospheric from shock to shock.

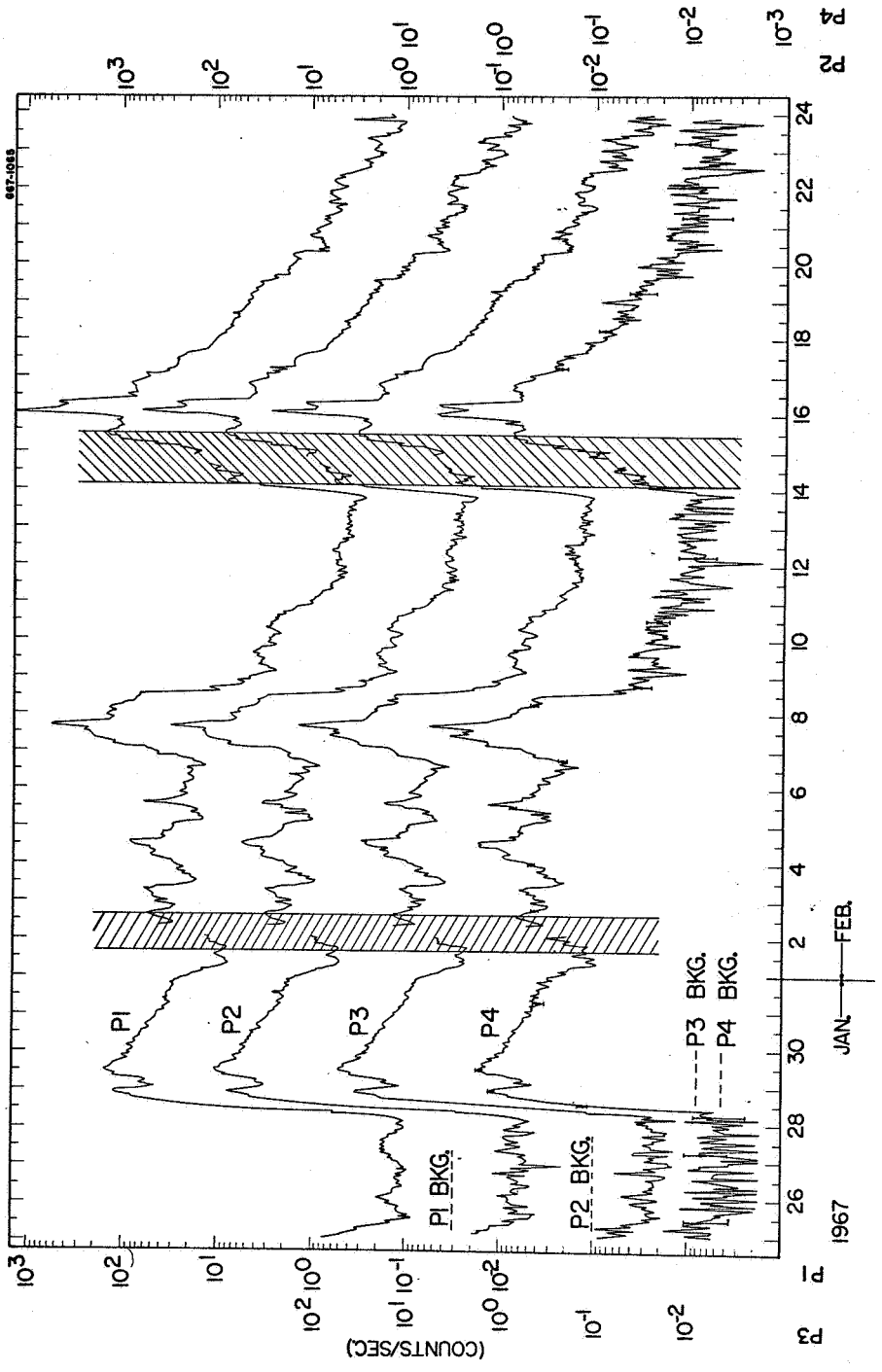

Figure 6

Figure 7 One-hour averages of the sectors of P1. The cross-hatched regions are magentospheric passages from shock to shock.

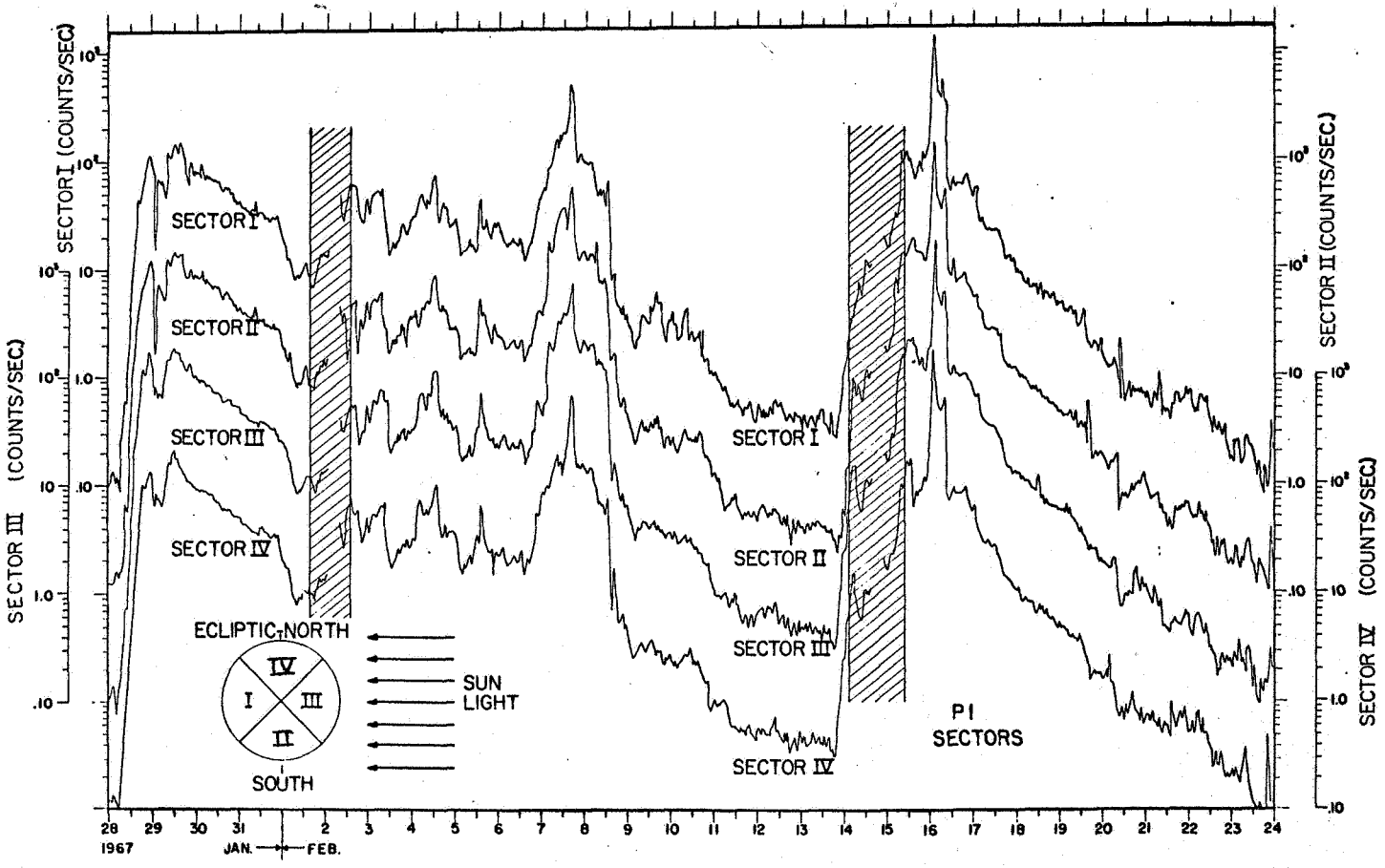
SECTOR I (COUNTS/SEC)
SECTOR II (COUNTS/SEC)
SECTOR III (COUNTS/SEC)
SECTOR IV (COUNTS/SEC)
SECTOR I
SECTOR II
SECTOR III
SECTOR IV
SECTOR I
SECTOR II
SECTOR III
SECTOR IV
P1
SECTORS
ECLIPTIC NORTH
SUN
LIGHT
SOUTH
I
II
III
IV
28 29 30 31 1 2 3 4 5 6 7 8 9 10 11 12 13 14 15 16 17 18 19 20 21 22 23 24
1967
JAN.
FEB.

Figure 8 Quarter-hour averages of the anisotropy parameters δ and C, where the anisotropy is assumed to be of the form $P1(\theta) = A[1 + C \cos(\theta + S)]$. The angles $\theta = 0°$, 90°, 180°, and 270° correspond to the directions anti-sun, ecliptic north and sunward, and ecliptic south, respectively.

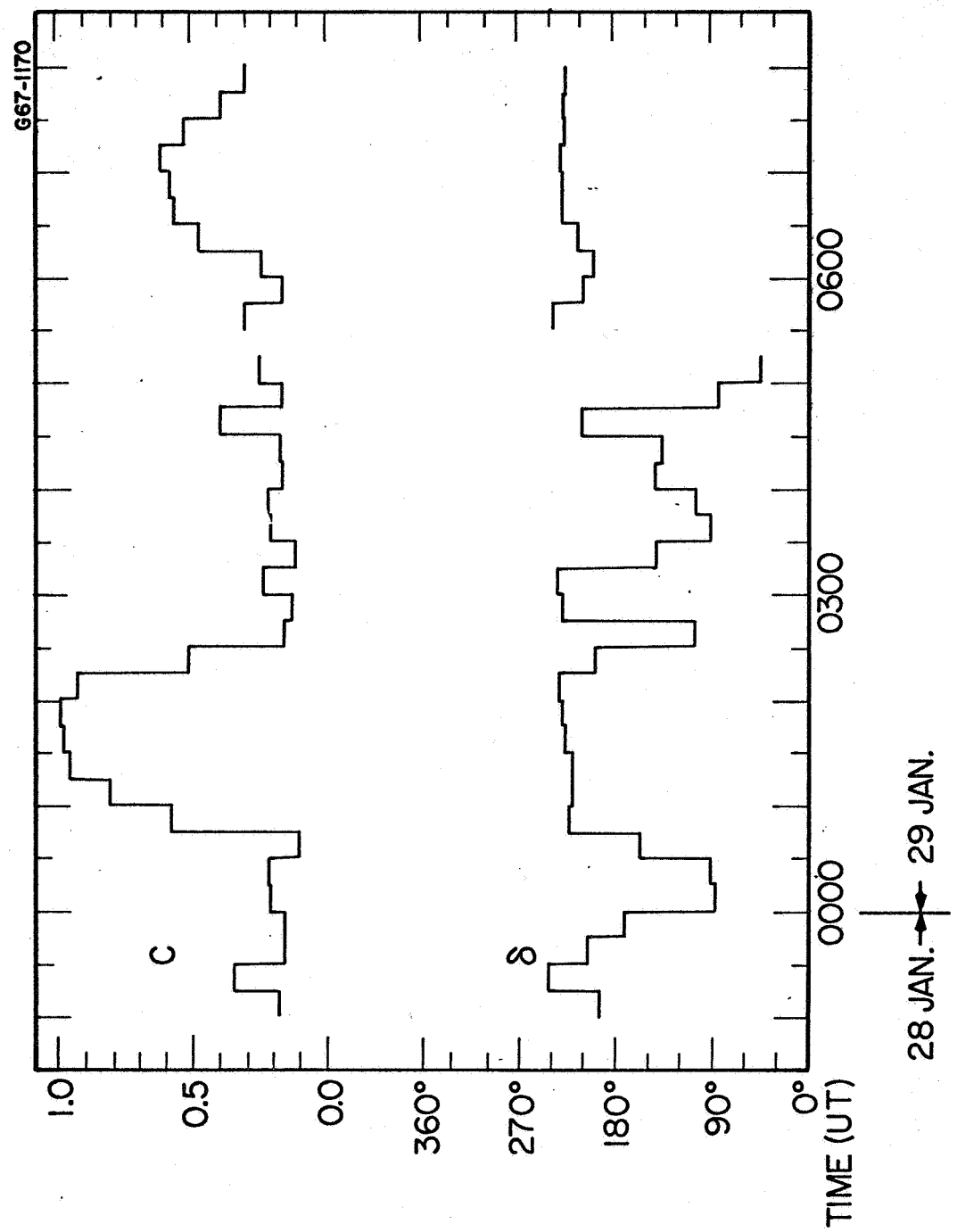
G67-1170
C
δ
1.0
0.5
0.0
360°
270°
180°
90°
0°
TIME (UT)
0000
0300
0600
28 JAN.
29 JAN.

Figure 8

Figure 9 The polar cap absorption (PCA) recorded by the Douglas 30 mc. riometer at McMurdo, Antartica [Masley and Goedeke, 1967]. The values of G1AV shown are one-hour averages. The crosshatched period is a magnetospheric passage of Explorer 33.

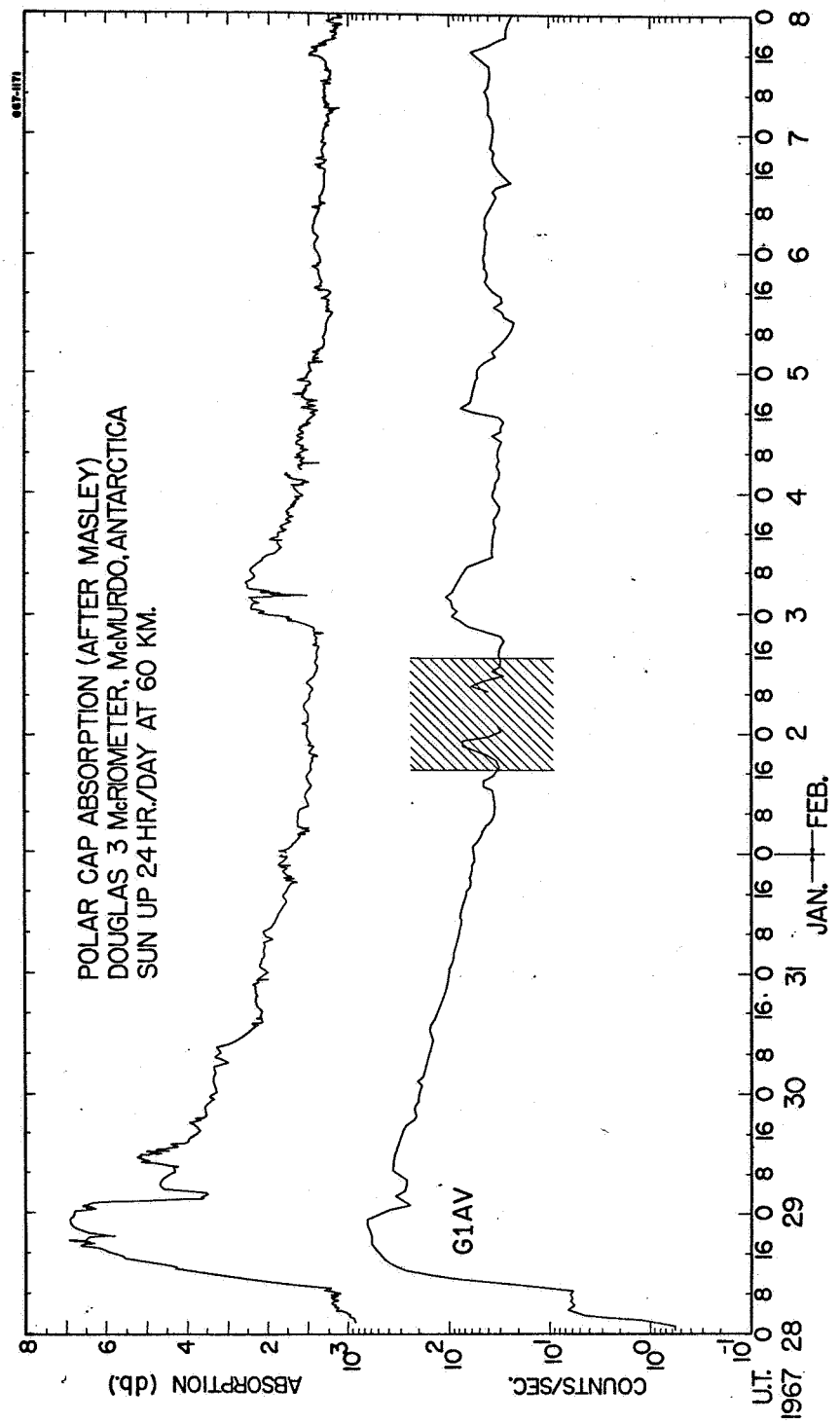
POLAR CAP ABSORPTION (AFTER MASLEY)
DOUGLAS 3 McRIOMETER, McMURDO, ANTARCTICA
SUN UP 24 HR./DAY AT 60 KM.
ABSORPTION (db.)
COUNTS/SEC.
G1AV
U.T.
1967
JAN.
FEB.

Figure 9

Figure 10 Neutron monitor one-hour sums. GlAV has been included for reference.

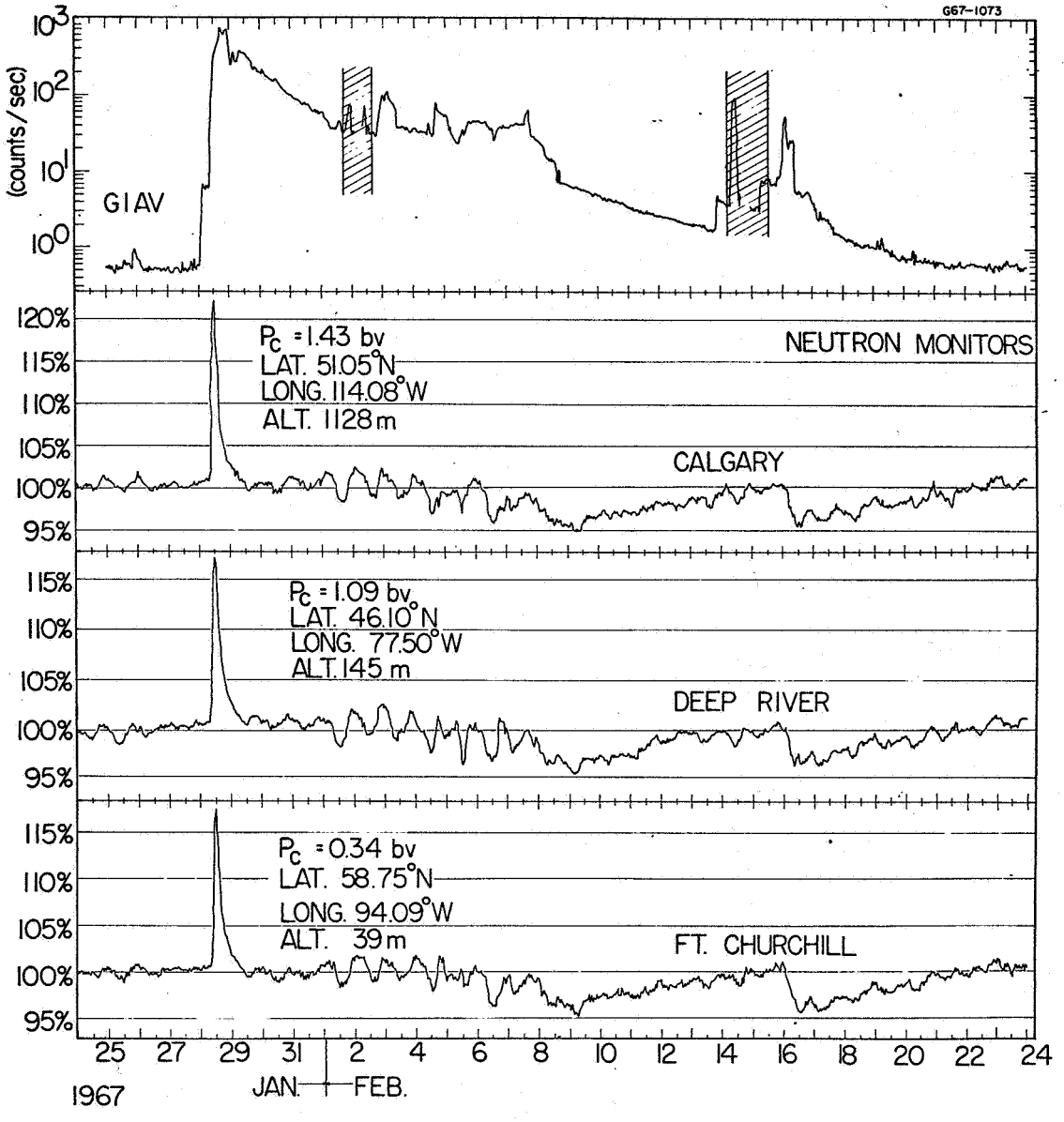
G67-1073
(counts/sec)
G1AV
NEUTRON MONITORS
Pc = 1.43 bv
LAT. 51.05°N
LONG. 114.08°W
ALT. 1128 m
CALGARY
Pc = 1.09 bv
LAT. 46.10°N
LONG. 77.50°W
ALT. 145 m
DEEP RIVER
Pc = 0.34 bv
LAT. 58.75°N
LONG. 94.09°W
ALT. 39 m
FT. CHURCHILL
1967
JAN.
FEB.

Figure 10

Figure 11 Five-minute averages for the Deep River neutron monitor increase of 28-29 January.

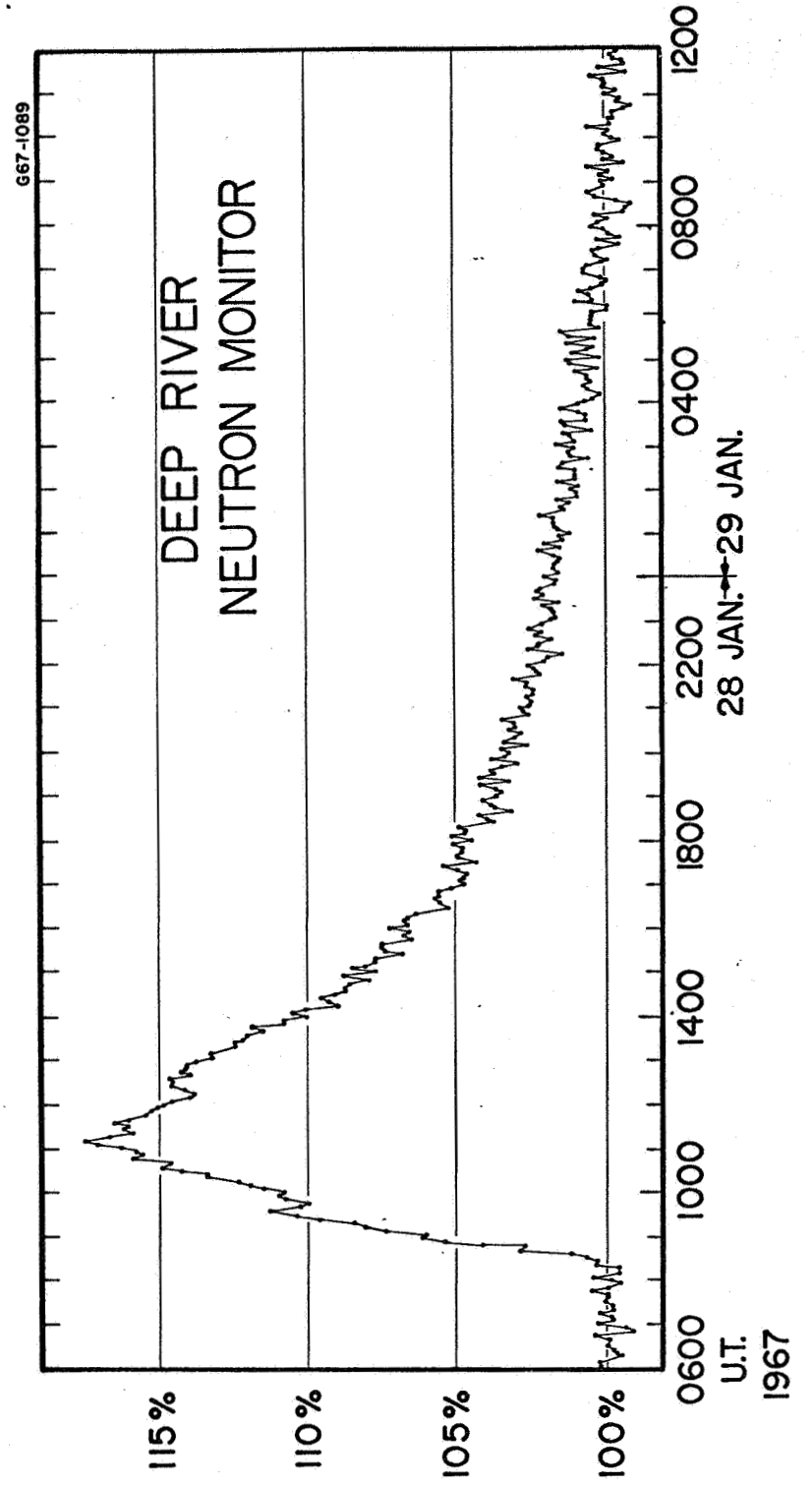
G67-1089
DEEP RIVER
NEUTRON MONITOR
115%
110%
105%
100%
0600
1000
1400
1800
2200
0400
0800
1200
U.T.
1967
28 JAN.
29 JAN.

Figure 11

Figure 12 Mariner IV data for 1642 UT to 2010 UT, 28 January. Some Explorer 33 data (G1AV, P2, and P3) have been included for comparison.

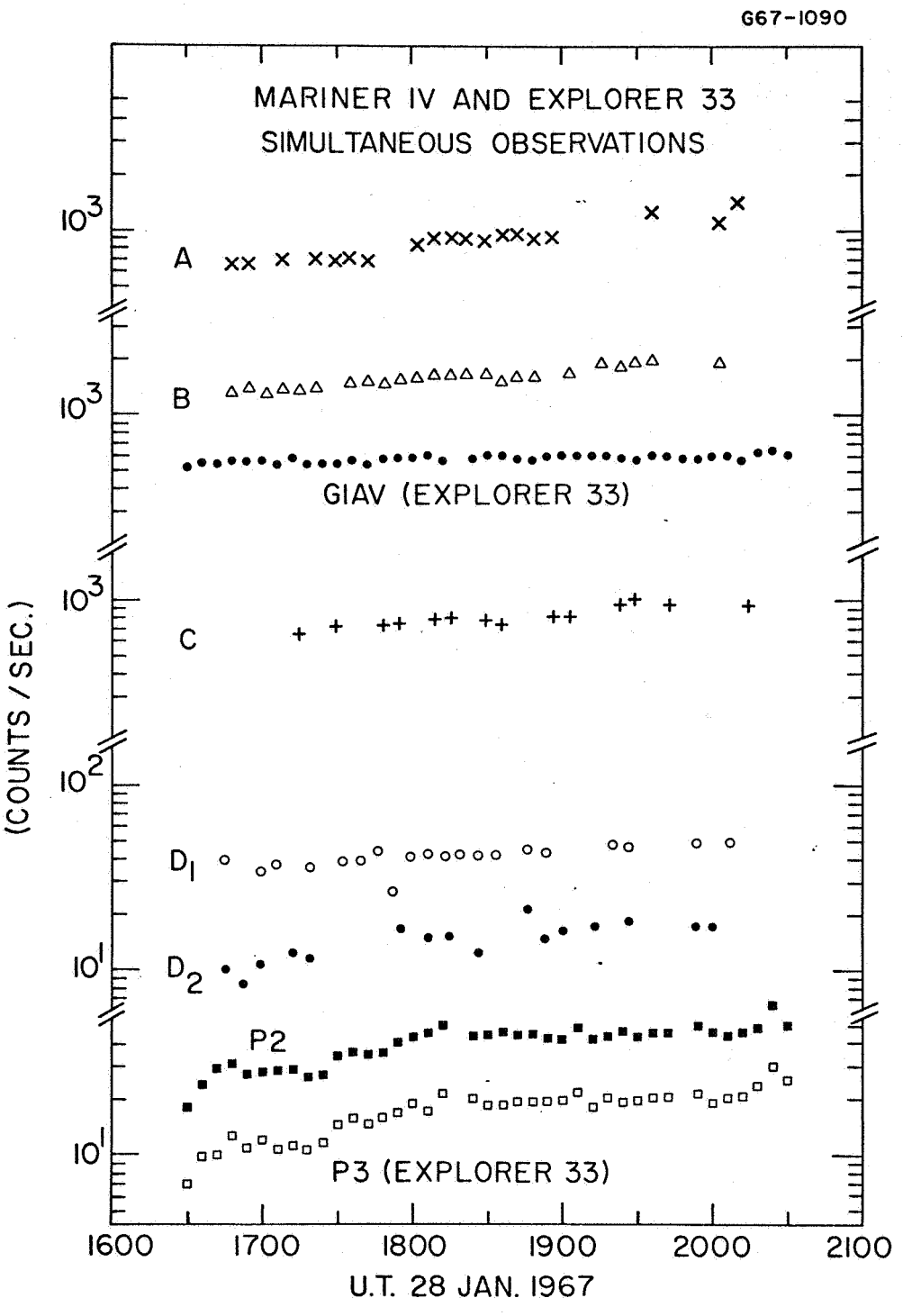
G67-1090
MARINER IV AND EXPLORER 33
SIMULTANEOUS OBSERVATIONS
A
B
GIAV (EXPLORER 33)
C
D1
D2
P2
P3 (EXPLORER 33)
(COUNTS / SEC.)
10^3
10^3
10^3
10^2
10^1
10^1
1600
1700
1800
1900
2000
2100
U.T. 28 JAN. 1967

Figure 12

Figure 13 The electron event of 2-3 February. Note the sudden decrease in both detectors. The data are half-hour averages. The three flares indicated are of importance 1-.

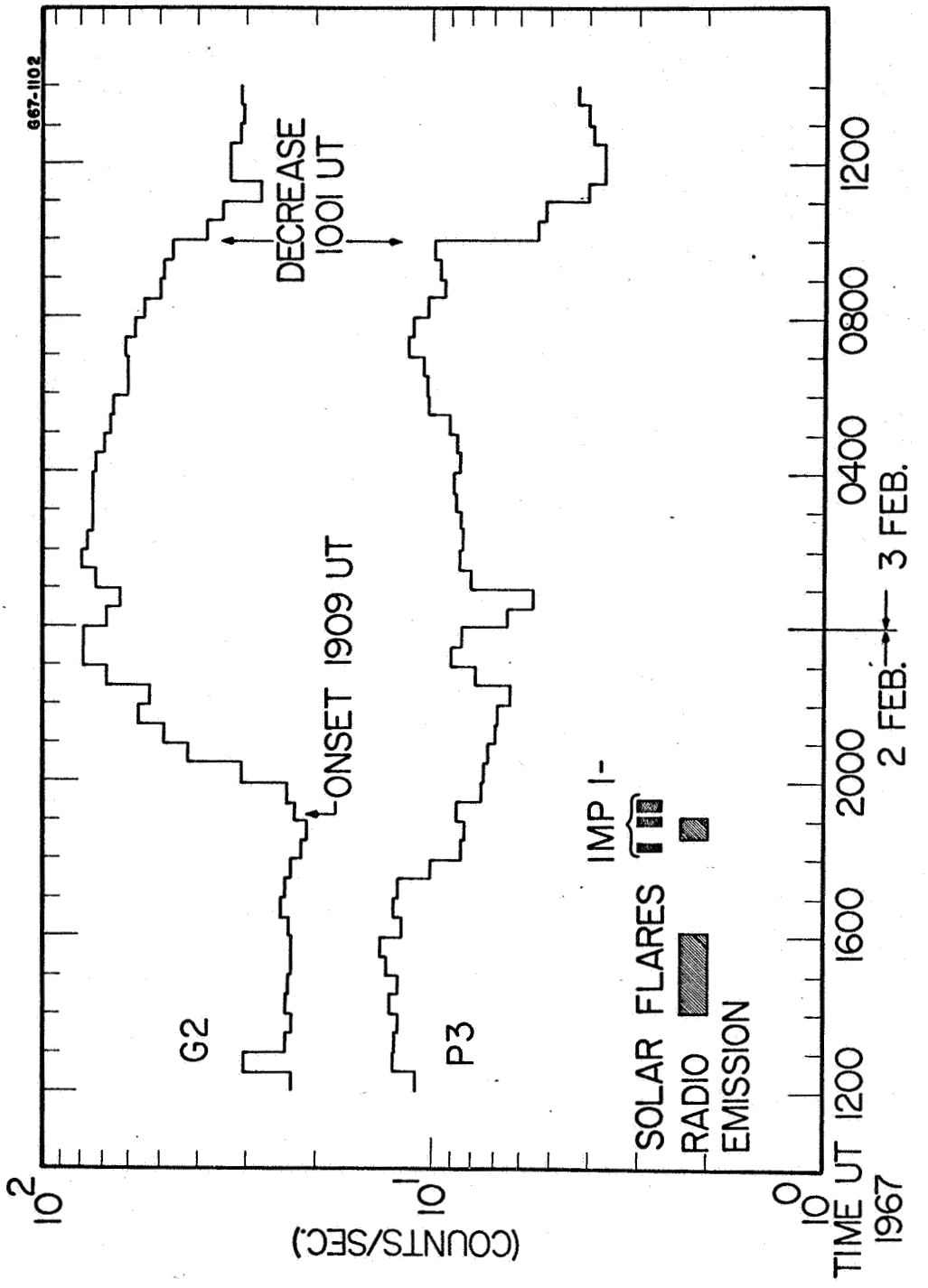
667-1102
DECREASE
1001 UT
ONSET 1909 UT
G2
P3
IMP I-
SOLAR FLARES
RADIO
EMISSION
10^2
10^1
10^0
(COUNTS/SEC.)
TIME UT 1200 1600 2000 0400 0800 1200
1967
2 FEB.
3 FEB.

Figure 13

Figure 14 Full detail data of the onset of the 4 February electron event. Note the dip in P3 that coincides with the onset of G2 and G1AV.

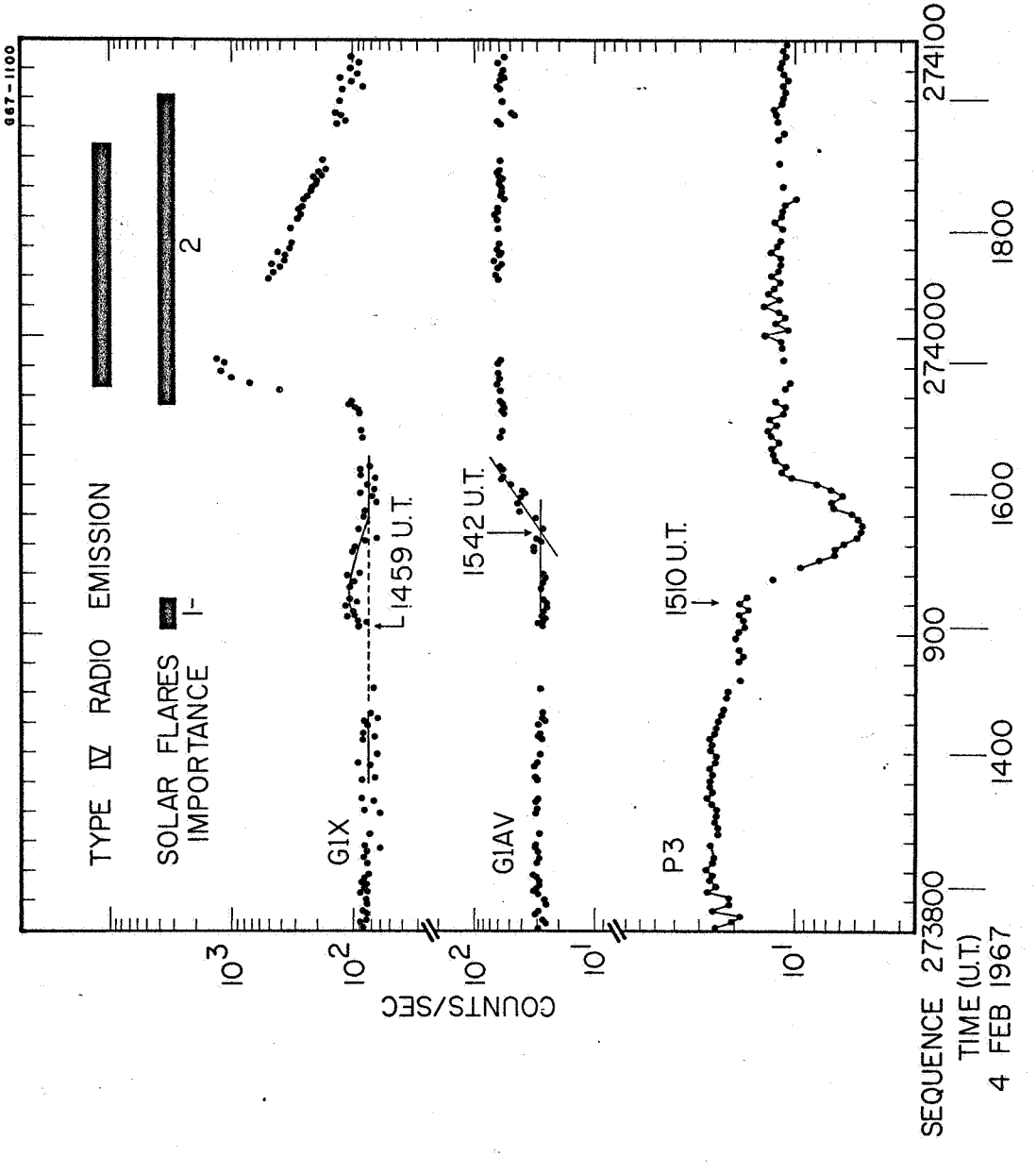
667-1100
TYPE IV RADIO EMISSION
SOLAR FLARES
IMPORTANCE
1-
2
G1X
1459 U.T.
1542 U.T.
G1AV
1510 U.T.
P3
COUNTS/SEC
10^3
10^2
10^2
10^1
10^1
SEQUENCE 273800
TIME (U.T.)
4 FEB 1967
1400
900
1600
274000
1800
274100

Figure 14

Figure 15 Half-hour averages of the 4-5 February electron event.

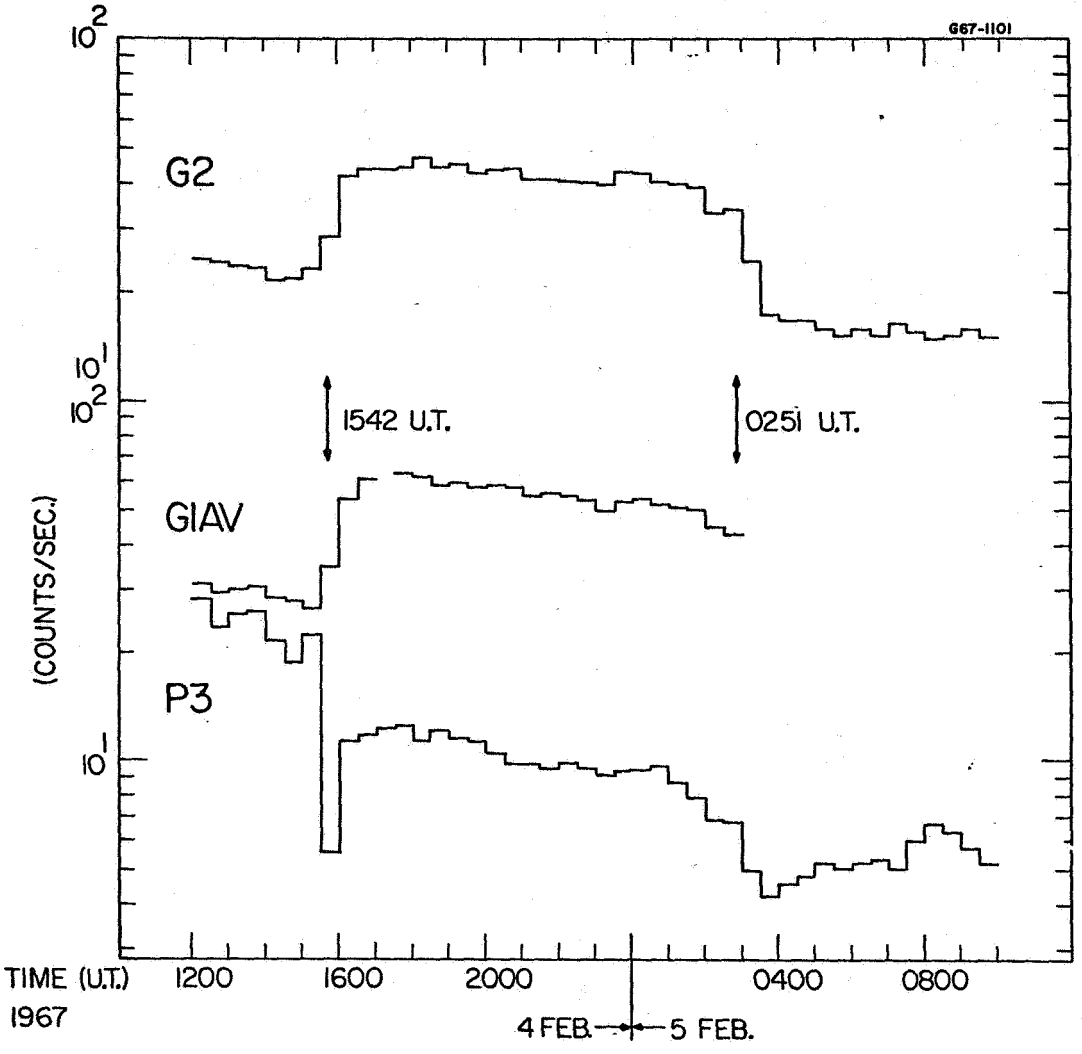
G67-1101
10^2
G2
10^1
10^2
1542 U.T.
0251 U.T.
GIAV
(COUNTS/SEC.)
P3
10^1
TIME (U.T.)
1967
1200
1600
2000
0400
0800
4 FEB.
5 FEB.

Figure 15

Figure 16 Full detail of the 13 February onset of G1X and G1AV.

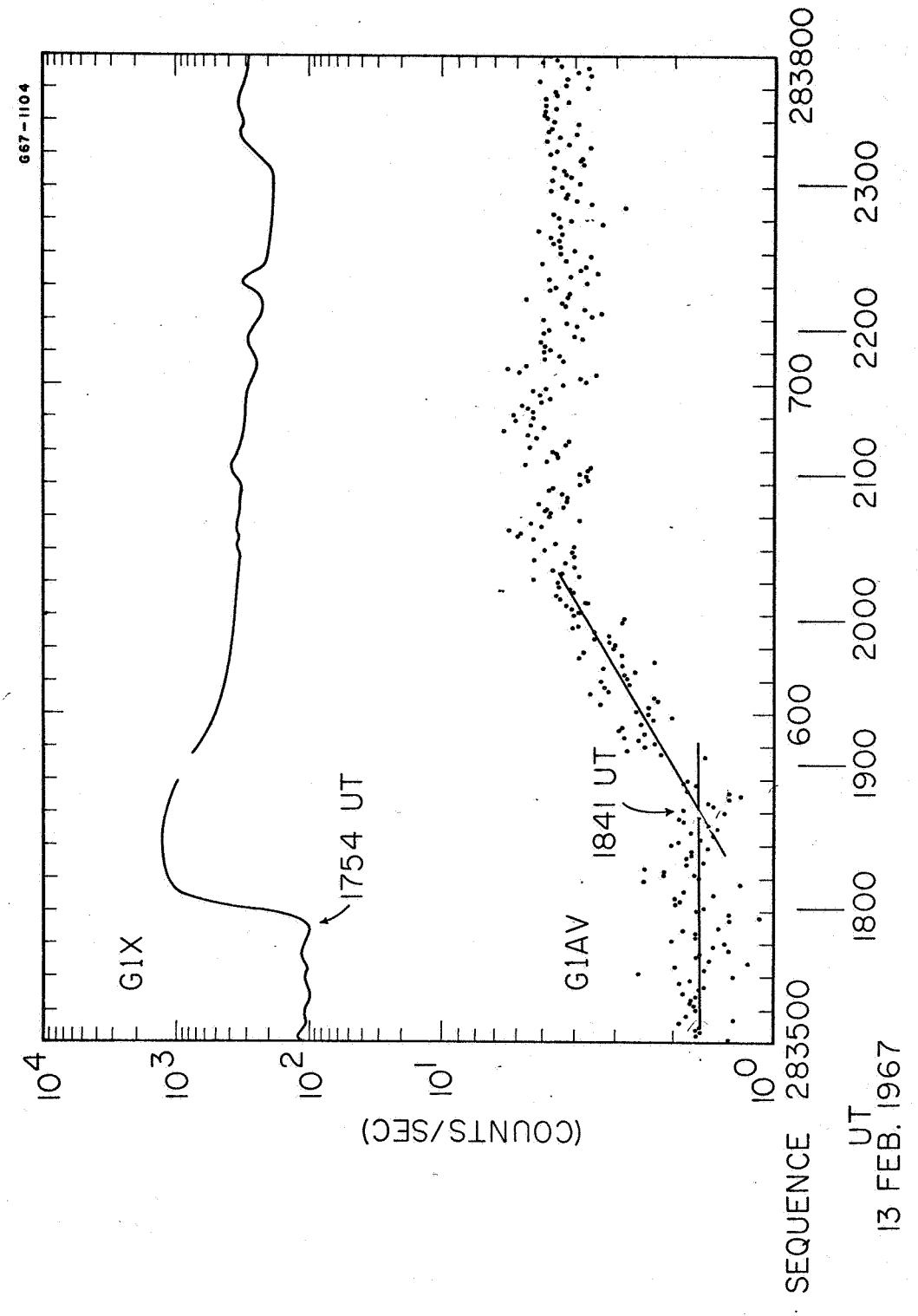
667-1104
G1X
1754 UT
G1AV
1841 UT
(COUNTS/SEC)
SEQUENCE
UT
13 FEB. 1967

Figure 16

Figure 17 Half-hour averages of the anisotropy parameters where δ and C are defined in Figure 7.

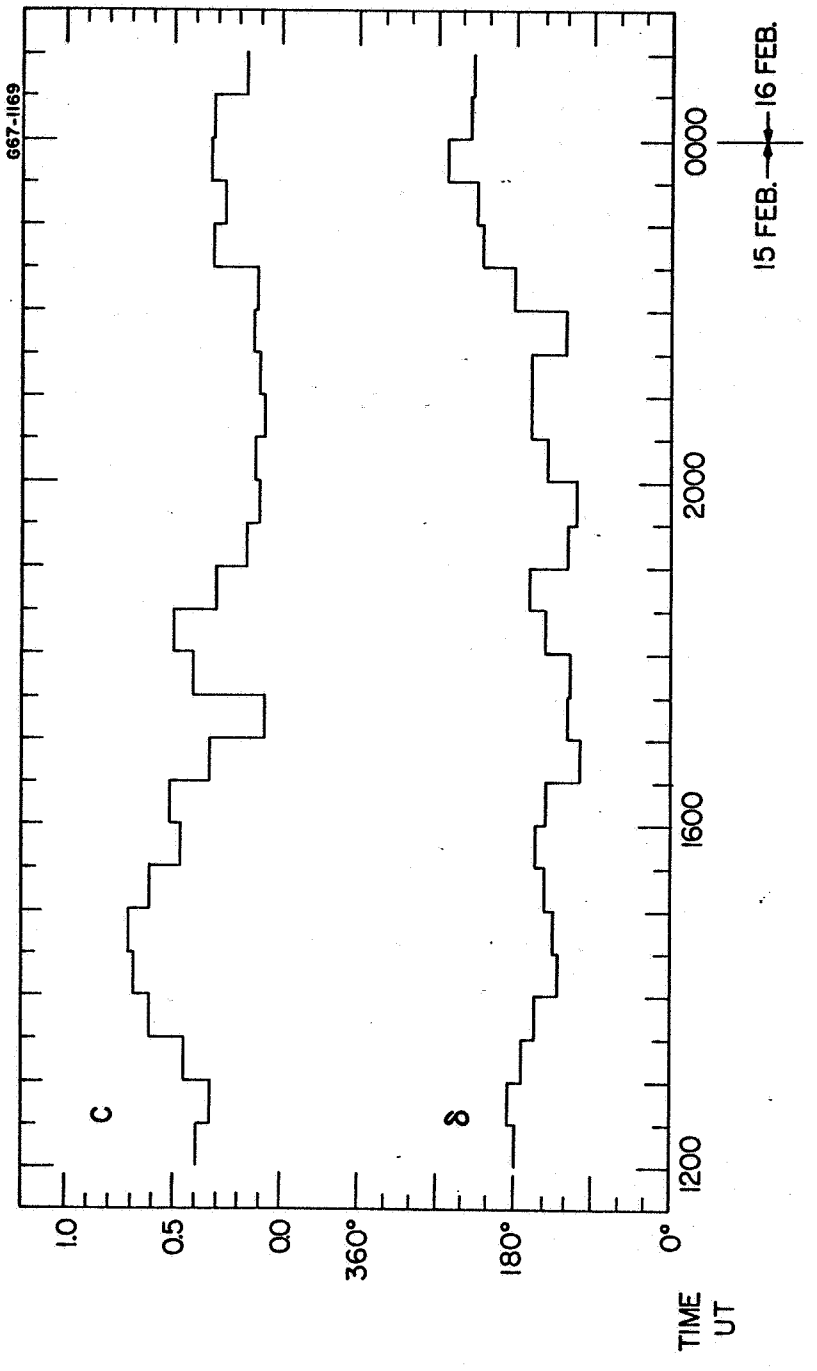
667-1169
15 FEB.
16 FEB.
0000
2000
1600
1200
TIME
UT
C
δ
1.0
0.5
0.0
360°
180°
0°

Figure 17

Figure 18 Full detail of the 16 February increase for G1X and G1AV.

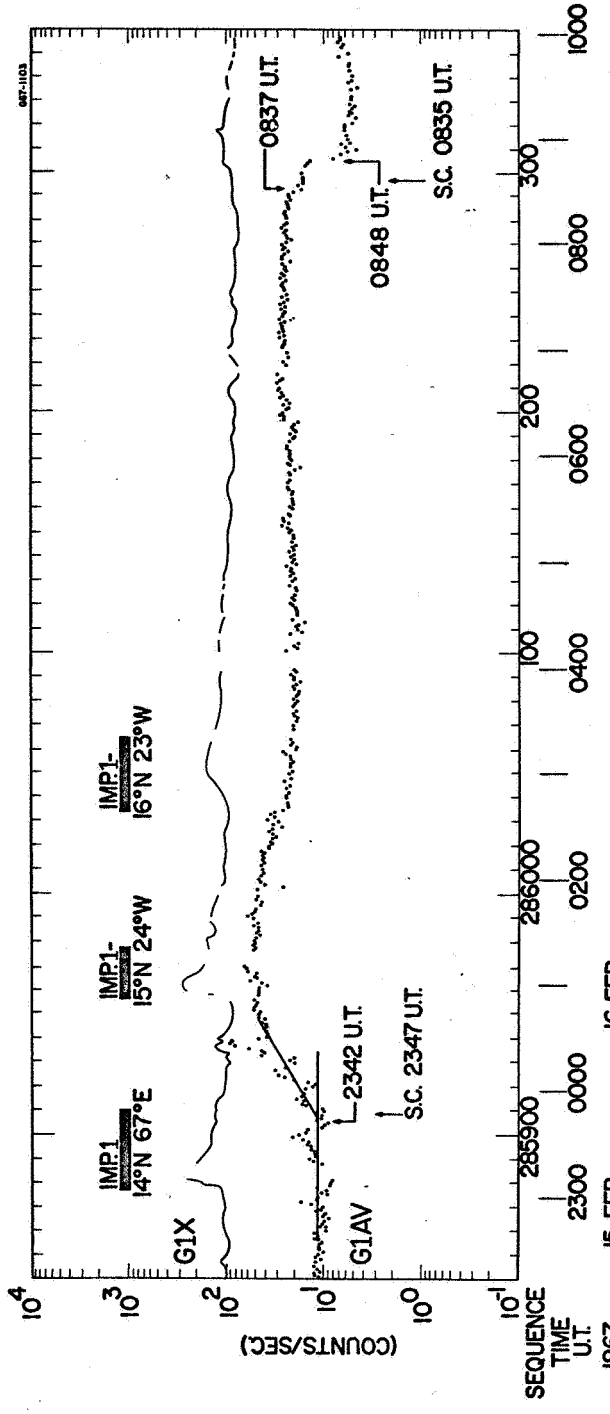
IMP 1
14°N 67°E
IMP 1
15°N 24°W
IMP 1
16°N 23°W
G1X
G1AV
2342 U.T.
S.C. 2347 U.T.
0837 U.T.
0848 U.T.
S.C. 0835 U.T.
(COUNTS/SEC)
SEQUENCE
TIME
U.T.
1967
15 FEB.
16 FEB.

Figure 18

Figure 19 The three-hour averages of the proton to alpha particle ratio for $0.5 \leq E/\text{nucleon} \leq 4.0$ MeV/nucleon. P2 is included for reference.

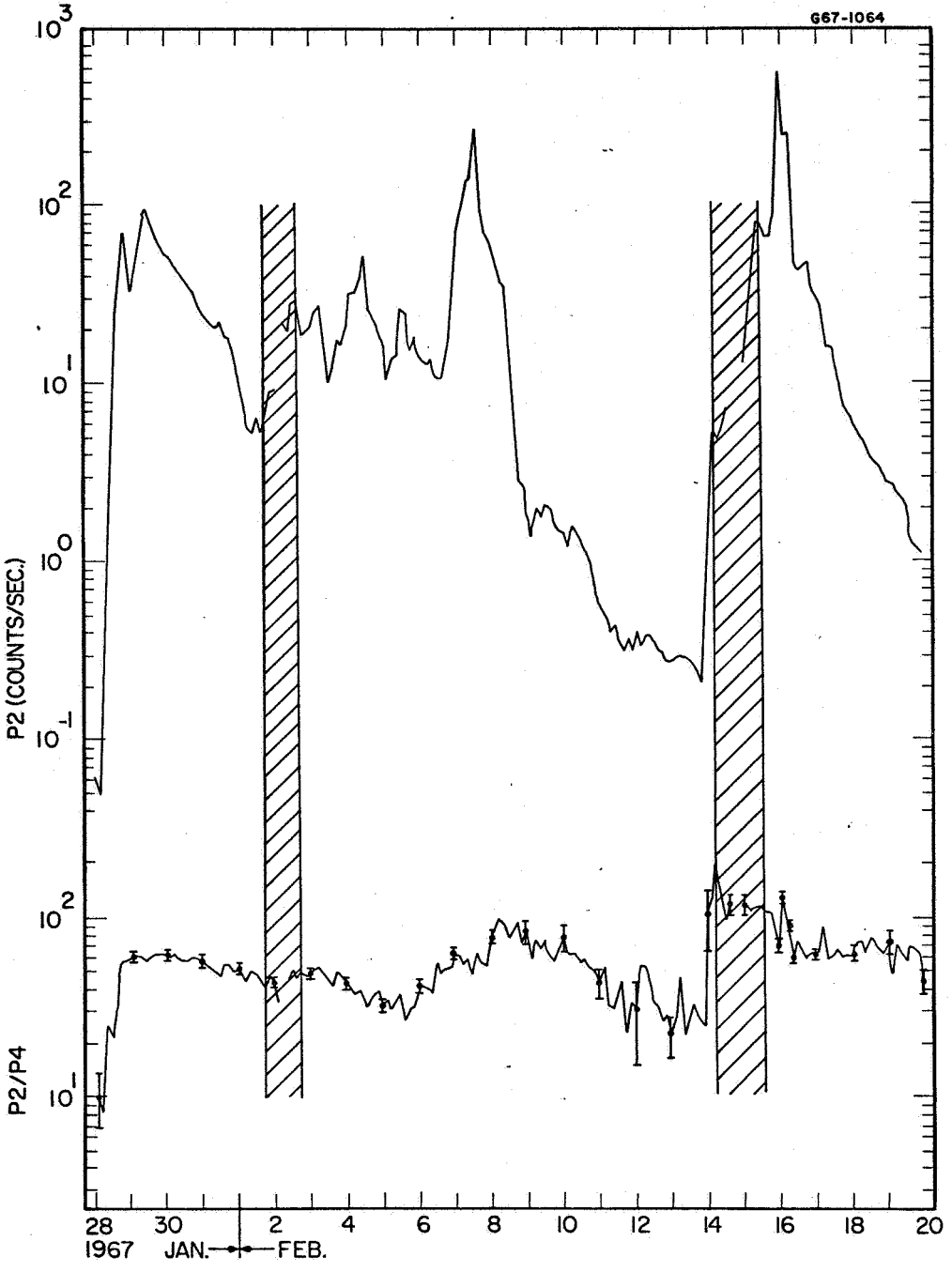
G67-1064
P2 (COUNTS/SEC.)
P2/P4
28
30
2
4
6
8
10
12
14
16
18
20
1967 JAN.
FEB.

Figure 19

Figure 20 Half-hour averages of the proton to alpha particle ratio peak in the 16 February increase. P2, P4, and the anisotropy parameters δ and C are included.

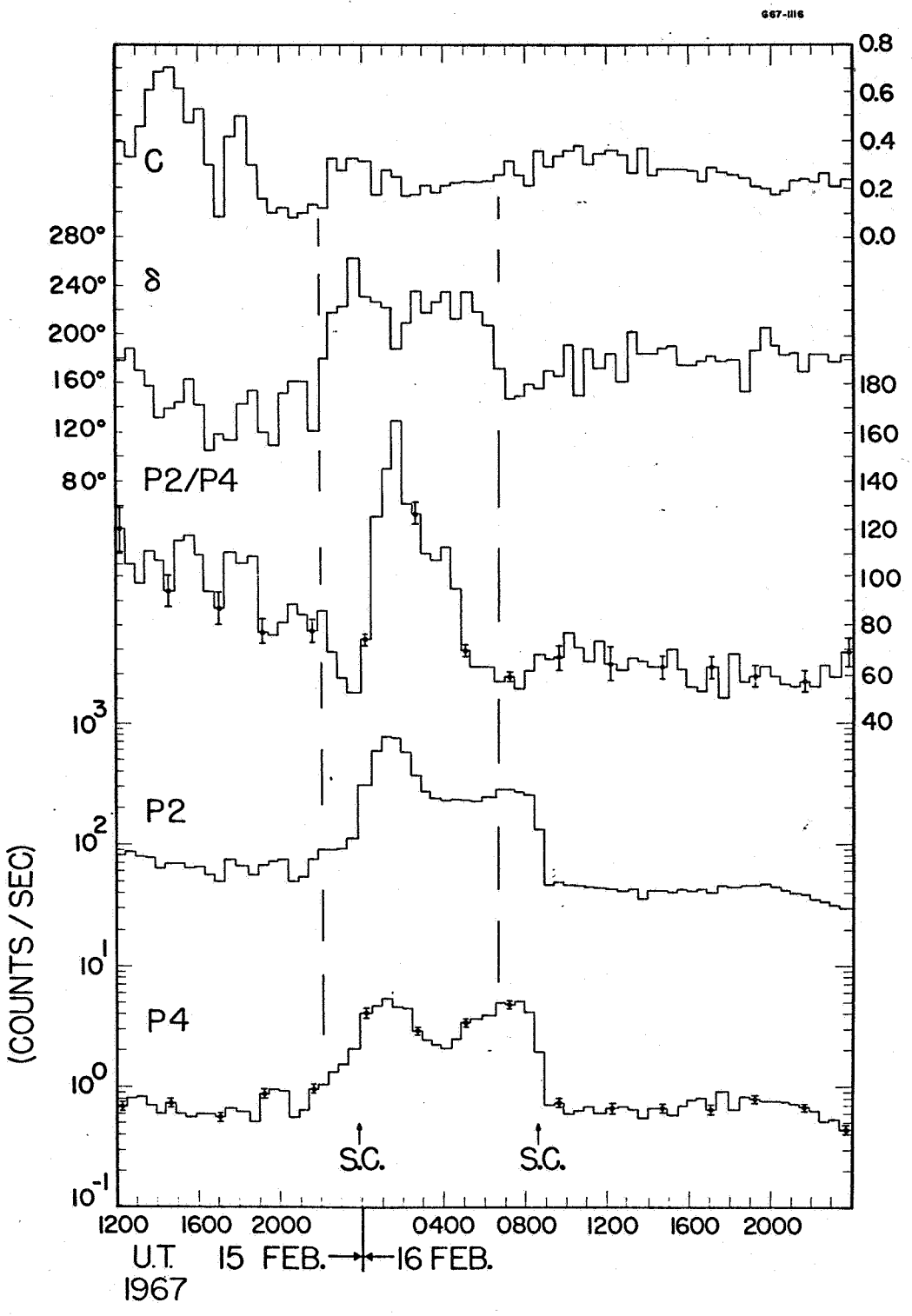
667-1116
C
δ
P2/P4
P2
P4
0.8
0.6
0.4
0.2
0.0
280°
240°
200°
160°
120°
80°
180
160
140
120
100
80
60
40
10^3
10^2
10^1
10^0
10^{-1}
(COUNTS / SEC)
S.C.
S.C.
1200
1600
2000
0400
0800
1200
1600
2000
U.T. 15 FEB. → ← 16 FEB.
1967

Figure 20

Figure 21 Active regions of the sun. This figure was compiled by extrapolaring the position of all flares from 1 January to 28 February of importance greater than 2- back (or forward) to their position on 28 January.

G67-1069

ACTIVE REGIONS OF THE SUN AT 0800 UT
28 JAN.

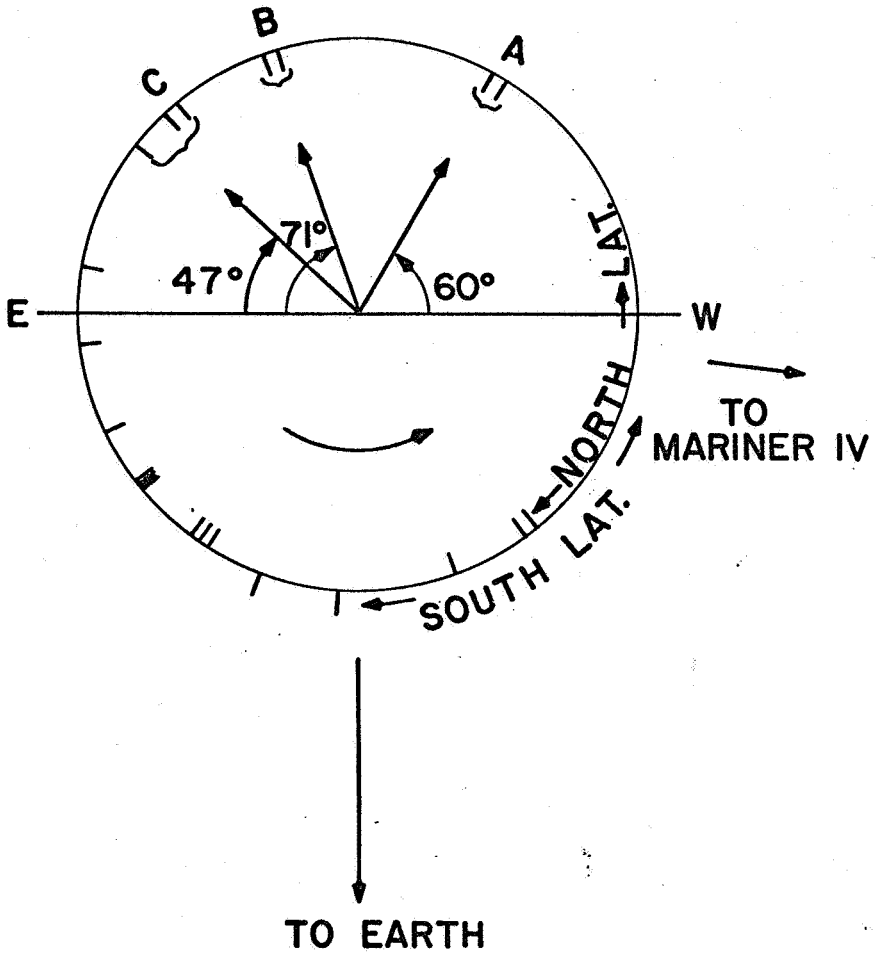

Figure 21

Figure 22 Analysis of the 28 January event using the diffusion model of Krimigis [1965]. The detector used is G1AV. Only data from 1100 to 2300 UT have been used.

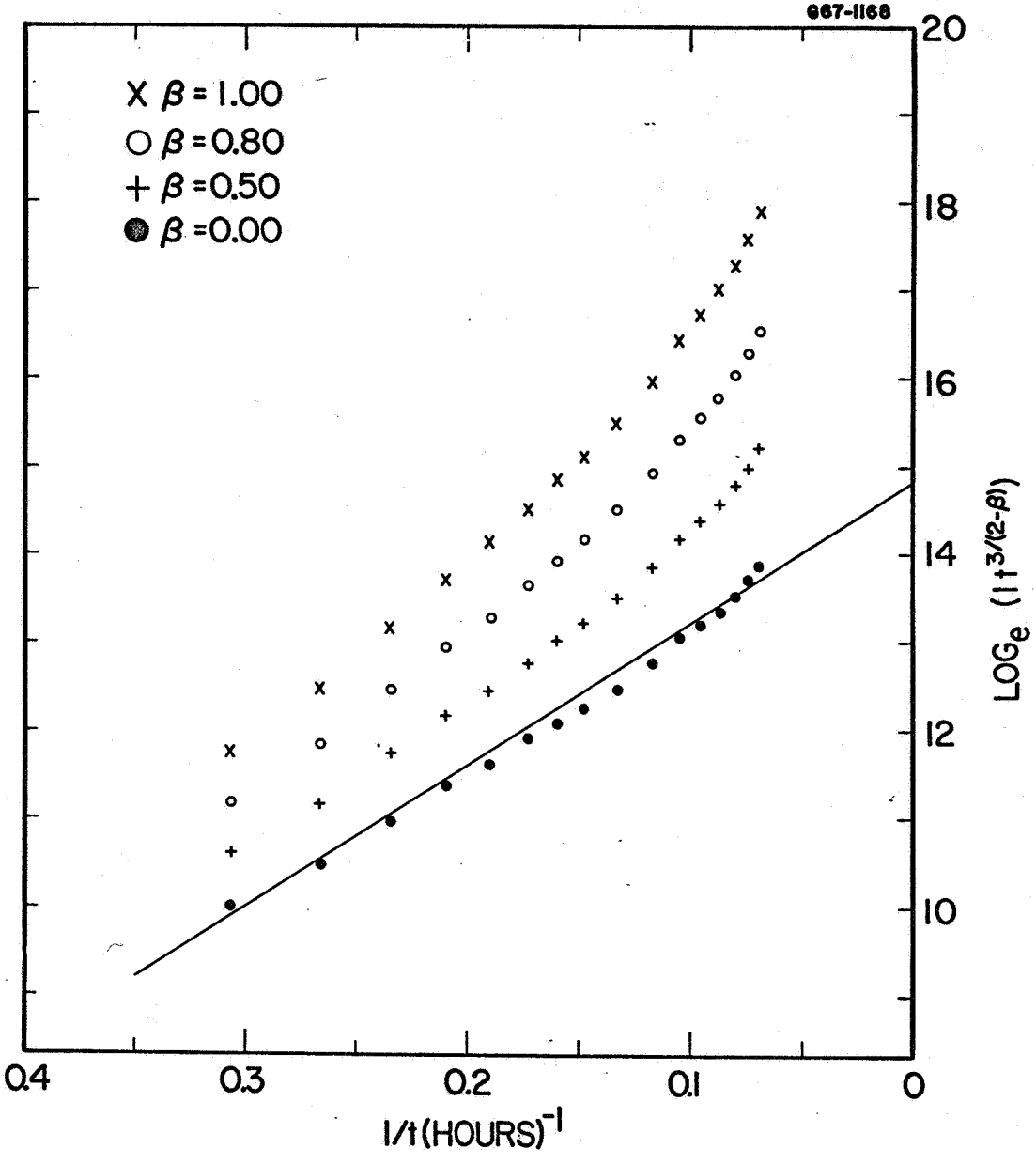
667-1168
X β = 1.00
○ β = 0.80
+ β = 0.50
● β = 0.00
20
18
16
14
12
10
0.4
0.3
0.2
0.1
0
1/t (HOURS)⁻¹
LOGe (1+t^3/(2-β))

Figure 22

Figure 23 The three ratios of the solid detector proton channels and the spectral parameter E_o of a falling exponential differential spectrum (see text). P1 is included for reference.

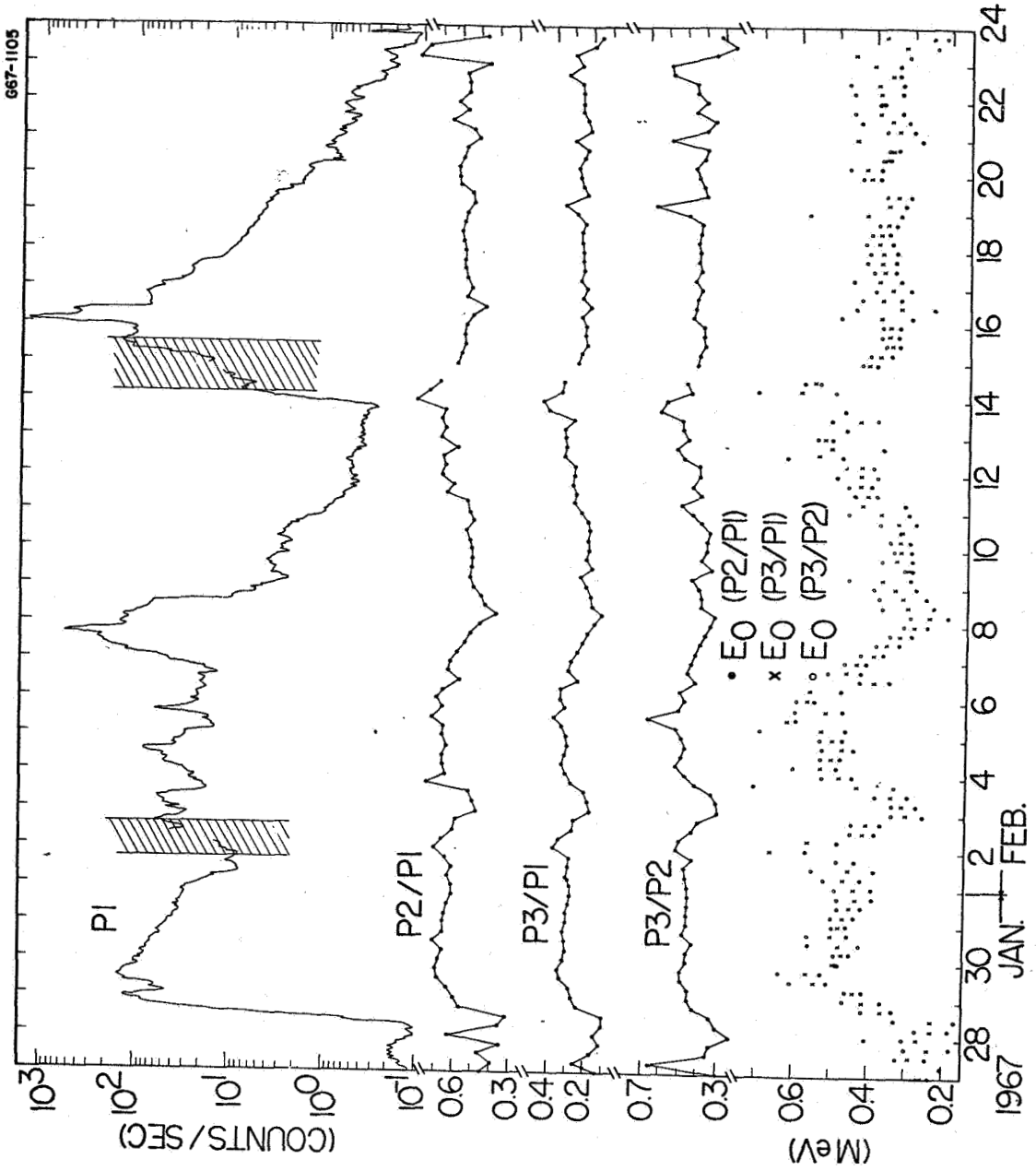
667-1105
P1
P2/P1
P3/P1
P3/P2
E0 (P2/P1)
E0 (P3/P1)
E0 (P3/P2)
(COUNTS/SEC)
(MeV)
JAN.
FEB.
1967

Figure 23